

The official publication of the
Hong Kong Academy of Medicine and
the Hong Kong Medical Association

HONG KONG

MEDICAL JOURNAL

香港醫學雜誌

26(3+4)

HONG KONG MEDICAL JOURNAL

香港醫學雜誌

Volume 26 Number 3 June 2020

Health and Medical Research Fund

Research Dissemination Reports

醫療衛生研究基金

研究成果報告

Respiratory Infection
呼吸道感染

Viral Hepatitis
病毒性肝炎

Helicobacter pylori
幽門螺桿菌

Bacterial Infection
細菌感染



MEDICAL JOURNAL

香港醫學雜誌

EDITOR-IN-CHIEF

Martin CS Wong 黃至生

SENIOR EDITORS

LW Chu 朱亮榮

Albert KK Chui 徐家強

Michael G Irwin

Eric CH Lai 賴俊雄

KY Leung 梁國賢

Anthony CF Ng 吳志輝

TW Wong 黃大偉

EDITORS

KS Chan 陳健生

Sherry KW Chan 陳喆燁

Jason PY Cheung 鍾培言

Kelvin KL Chong 莊金隆

Jacqueline PW Chung 鍾佩樺

James TK Fung 馮德焜

Brian SH Ho 何思灝

Ellis KL Hon 韓錦倫

Junjie Huang 黃俊杰

KW Huang 黃凱文

WK Hung 熊維嘉

Bonnie CH Kwan 關清霞

Ho Lam 林賀

Arthur CW Lau 劉俊穎

PY Lau 婁培友

Danny WH Lee 李偉雄

Thomas WH Leung 梁慧康

WK Leung 梁惠強

Kenneth KW Li 李啟煌

Janice YC Lo 羅懿之

Herbert HF Loong 龍浩鋒

James KH Luk 陸嘉熙

Arthur DP Mak 麥敦平

Henry KF Mak 麥嘉豐

Martin W Pak 白威

Walter WK Seto 司徒偉基

Regina WS Sit 薛詠珊

William YM Tang 鄧旭明

Jeremy YC Teoh 張源津

KY Tse 謝嘉瑜

Harry HX Wang 王皓翔

HL Wong 黃學良

Kenneth KY Wong 黃格元

Patrick CY Woo 胡釗逸

Hao Xue 薛浩

Jason CS Yam 任卓昇

Bryan PY Yan 甄秉言

TK Yau 游子覺

Kelvin KH Yiu 姚啟恒

EPIDEMIOLOGY ADVISERS

Daniel SY Ho 何世賢

Eman Leung 梁以文

Edmond SK Ma 馬紹強

Gary Tse 謝家偉

Shelly LA Tse 謝立亞

Ian YH Wong 王逸軒

Esther YT Yu 余懿德

Hunter KL Yuen 袁國禮

STATISTICAL ADVISERS

Marc KC Chong 莊家俊

William B Goggins

Eddy KF Lam 林國輝

Carlos KH Wong 黃競浩

HONORARY ADVISERS

David VK Chao 周偉強

Paul BS Lai 賴寶山

Health and Medical Research Fund**Research Dissemination Reports****Editorial**

3

RESPIRATORY INFECTION**Efficacy of face masks to prevent respiratory virus transmission: abridged secondary publication**

4

*BJ Cowling, DK Ip, HL Yen***Human parechovirus infection in Hong Kong neonates, infants, and young children: abridged secondary publication**

8

*PKS Chan, MCW Chan, EAS Nelson, TF Leung***Effect of increased influenza and pneumococcal vaccine coverage on the burden of influenza among elderly people in Hong Kong versus Brisbane: abridged secondary publication**

12

*L Yang, WB Hu, CM Wong, SSS Chiu, RJ Soares Magalhaes, TQ Thach, ACA Clements, JSM Peiris***Severity profiles of respiratory viruses in children in Hong Kong: abridged secondary publication**

17

*P Wu, BJ Cowling, JSM Peiris***VIRAL HEPATITIS****C-terminal truncated hepatitis B virus X protein regulates tumorigenicity, self-renewal, and chemoresistance via STAT3/Nanog signalling pathway: abridged secondary publication**

22

*RHH Ching, KMF Sze, EYT Lau, YT Chiu, JMF Lee, IOL Ng, TKW Lee***HELICOBACTER PYLORI****Involvement of autophagy in antibacterial actions of vitamin D in *Helicobacter pylori* infection: abridged secondary publication**

26

*W Hu, L Zhang, WKK Wu, CH Cho***Structure-based discovery of inhibitors of *Helicobacter pylori* urease: abridged secondary publication**

29

*CL Tam, MH Yuen, YS Nim, YF Xu, SWN Au, JCK Ngo, P Huang, KB Wong***Role of HP1076 in type IV secretion pathway in *Helicobacter pylori*: abridged secondary publication**

32

WL Lam, M Li, KF Lau, VSF Chan, SWN Au

**INTERNATIONAL EDITORIAL
ADVISORY BOARD**

Sabaratnam Arulkumaran
United Kingdom
Robert Atkins
Australia
Peter Cameron
Australia
Daniel KY Chan
Australia
David Christiani
United States
Andrew Coats
Australia
James Dickinson
Canada
Willard Fee, Jr
United States
Robert Hoffman
United States
Roger Jones
United Kingdom
Michael Kidd
Australia
Arthur Kleinman
United States
Stephen Leeder
Australia
Xiaoping Luo
PR China
William Rawlinson
Australia
Jonathan Samet
United States
Yaojiang Shi
PR China
David Weller
United Kingdom
Max Wintermark
United States
Wanghong Xu
PR China
Atsuyuki Yamataka
Japan
Homer Yang
Canada
KG Yeoh
Singapore
Matthew Yung
United Kingdom
Zhijie Zheng
PR China

Full details of the Editorial Board
are available online at
<https://www.hkmj.org/about/eo.html>

BACTERIAL INFECTION

Characterisation of <i>Staphylococcus aureus</i> virulence factor EsxA and structure-based screening of EsxA inhibitors for combating methicillin-resistant <i>S aureus</i>: abridged secondary publication <i>KH Sze, RYT Kao</i>	35
Genomic and transcriptomic analyses of the <i>Salmonella</i> virulence network: abridged secondary publication <i>MHY Wong, D Lin, R Li, EWC Chan, S Chen</i>	39
Molecular mechanisms of fluoroquinolone and expanded-spectrum cephalosporin resistance in <i>Vibrio parahaemolyticus</i>: abridged secondary publication <i>S Chen, EWC Chan, KHL Po, L Ye, R Li</i>	43
Author index & Disclaimer	48

MANAGING EDITOR

Alan Purvis

DEPUTY MANAGING EDITOR

Betty Lau 劉薇薇

ASSISTANT MANAGING EDITOR

Warren Chan 陳俊華

Editorial

Dissemination reports are concise informative reports of health-related research supported by the Health and Medical Research Fund (and its predecessor funds) administered by the Food and Health Bureau. In this edition, we present 11 dissemination reports of projects related to respiratory infection, viral hepatitis, *Helicobacter pylori*, and bacterial infection. In particular, three projects are highlighted due to their potentially significant findings, impact on healthcare delivery and practice, and/or contribution to health policy formulation in Hong Kong.

The burden caused by respiratory virus infections includes hospitalisation and death as well as economic losses due to sick leave and doctor consultations. Respiratory viruses can be transmitted by contact, large droplets, and aerosols. Cowling et al¹ aimed to detect respiratory virus RNA from the exhaled breath of persons infected with one of a range of common respiratory infections and to determine the potential benefits of face masks to prevent respiratory virus transmission. The investigators found that respiratory viruses could be detected in exhaled breath of patients with acute respiratory infections. Overall, respiratory viruses were less frequently detected in exhaled breath in the group wearing surgical masks when compared with the control group in the aerosol (7% vs 13%) and droplet (0% vs 6%) fractions. Surgical masks were effective in preventing virus dissemination in the coarse fraction of exhaled breath even when a participant coughed many times.

Human parechovirus (HPeV) is a virus common in Europe and some Asian countries. HPeV exists as 16 different strains that cause mainly respiratory and gastrointestinal symptoms. Chan et al² set out to determine its prevalence, seasonality, and clinical profile among young children aged 3 months and

under hospitalised for acute viral illness. They found that HPeV infection occurred in about 2.3% of young children hospitalised for acute viral illnesses with most infections occurring in autumn and winter. Symptoms ranged from mild gastroenteritis, upper respiratory tract infection, febrile rash to convulsion and severe sepsis. The authors suggested that a diagnostic service for HPeV might be useful for young infants presenting with sepsis.

Influenza infection is associated with a heavy burden of mortality and morbidity globally, and vaccination is an important strategy to reduce disease severity and virus transmission. However, the true effectiveness of influenza vaccines in older people is subject to debate. Yang et al³ compared the long-term trend of influenza burden in older people aged ≥65 years in Hong Kong and Brisbane and aimed to quantify the impact of influenza and pneumococcal vaccine coverage on the reduction of influenza disease burden. They found that the uptake of both vaccines had increased dramatically in Hong Kong since 2003. In the period 2003-2009 in Hong Kong, influenza-associated rates of mortality secondary to cardio-respiratory disease, stroke, and ischaemic heart disease decreased more in Hong Kong than in Brisbane. This provides some evidence to suggest that increased vaccination rates have reduced influenza disease burden in older people in Hong Kong.

We hope you will enjoy this selection of research dissemination reports. Electronic copies of these dissemination reports and the corresponding full reports can be downloaded individually from the Research Fund Secretariat website (<https://rfs2.fhb.gov.hk/>). Researchers interested in the funds administered by the Food and Health Bureau may visit the website for detailed information about application procedures.

Supplement editor



Dr Richard A Collins
Chief Scientific Reviewer
(Research Office)
Food and Health Bureau

References

1. BJ Cowling, DK Ip, HL Yen. Efficacy of face masks to prevent respiratory virus transmission: abridged secondary publication. *Hong Kong Med J* 2020;26(Suppl 4):S4-7.
2. PKS Chan, MCW Chan, EAS Nelson, TF Leung. Human parechovirus infection in Hong Kong neonates, infants, and young children: abridged secondary publication. *Hong Kong Med J* 2020;26(Suppl 4):S8-11.
3. L Yang, WB Hu, CM Wong, et al. Effect of increased influenza and pneumococcal vaccine coverage on the burden of influenza among elderly people in Hong Kong versus Brisbane: abridged secondary publication. *Hong Kong Med J* 2020;26(Suppl 4):S12-6.

Efficacy of face masks to prevent respiratory virus transmission: abridged secondary publication

BJ Cowling *, DK Ip, HL Yen

KEY MESSAGES

1. Various respiratory viruses can be detected in exhaled breath of patients with acute respiratory infections.
2. Viral loads are greatest in those with influenza virus infection.
3. We did not identify a significant effect of surgical face masks in reducing the amount of respiratory virus detected in coarse or fine particles in

exhaled breath.

Hong Kong Med J 2020;26(Suppl 4):S4-7

HMRF project number: 13120592

BJ Cowling, DK Ip, HL Yen

School of Public Health, The University of Hong Kong, Hong Kong

* Principal applicant and corresponding author: bcowling@hku.hk

Introduction

Respiratory viruses cause infections and hence economic losses through sick leave and doctor consultations as well as hospitalisations and deaths. The most severe acute upper respiratory tract infections are usually due to respiratory syncytial virus (RSV) in infants and influenza in all ages. The burden of other common respiratory viruses (parainfluenza, adenovirus, metapneumovirus, coronavirus, and rhinovirus) is also considerable. These viruses often result in a broad and overlapping spectrum of symptoms collectively referred to as common cold.

Modes of respiratory virus transmission include contact, large droplets, and aerosols. Although hand hygiene and use of face masks, primarily targeting contact and large droplet transmission, have been suggested as mitigation strategies against influenza virus, little is known about the relative importance of these modes to transmission for other common respiratory viruses apart from influenza. It has been suggested that contact transmission predominates for RSV, whereas both contact and aerosol transmissions are possible for rhinovirus.

There are a few studies reporting recovery of non-influenza respiratory viruses from human exhaled breath or aerosol samples from clinics. During the SARS epidemic in 2003, most Hong Kong people wore face masks. Although one study suggested that public health interventions during the SARS epidemic were effective in preventing other respiratory virus transmissions, little is known about the efficacy of face masks in filtering respiratory virus from an individual with respiratory infections. Most of the existing evidence on the filtering efficacy of face masks and respirators come from *in vitro* experiments that mainly use non-biological

particles that may not be generalisable to infectious respiratory virus droplets. There are few *in vivo* studies investigating the efficacy of face masks and quantifying viral titres and virus generation rates in human exhaled breath aerosols.

This study aimed to examine exhaled breath virus generation rate of different respiratory viruses (with implications for modes of transmission) and to determine the potential benefits of face masks to prevent respiratory virus transmission.

Methods

This study was approved by the Institutional Review Board of the University of Hong Kong. Written informed consent was obtained from all patients and from parents or legal guardians of patients aged 11 to 17 years.

From April 2014 to March 2016, we recruited local residents aged ≥ 11 years who reported at least two signs or symptoms of acute respiratory illness within 72 hours of illness onset from a local outpatient clinic in Hong Kong outside influenza seasons. A set of nose and throat swab sample was collected. Subjects were invited to do a short questionnaire to record demographic information including age, sex, clinical illness symptoms, medication used, and medical, allergy, and smoking history.

Subjects were asked to tidally breathe to the G-II bioaerosol collective device for at least 30 minutes while wearing a surgical face mask (Kimberley Clark). The G-II would collect their exhaled breath aerosol particles into two different size fractions, either with aerodynamic diameter $\geq 5 \mu\text{m}$ or $< 5 \mu\text{m}$, by the sample impactor and collection fluid (viral transport reservoir buffer), respectively. Then, the sample impactor and collection fluid from the G-II were collected and

changed. Finally, the subjects were asked to tidally breathe again to the G-II bioaerosol collective device for at least 30 minutes, without wearing a face mask.

The nasal and throat swabs were placed in viral transport media refrigerated at 2°C to 8°C immediately after collection, stored at -20°C for up to 7 days, and then stored at -80°C until testing qualitatively for the presence of respiratory viruses by the xTAG Respiratory Viral Panel, and subsequently quantitatively by RT-PCR. The exhaled droplets from subjects captured by bioaerosol collector G-II in $\geq 5\text{-}\mu\text{m}$ fraction collected on the impactor plate were stored in a 50 mL tube, and exhaled droplets in $< 5\text{-}\mu\text{m}$ fractions collected in 150 mL viral transport reservoir buffer, were refrigerated at 2°C to 8°C immediately after collection and stored at 4°C during transport. Once in the laboratory, the impactor plate was swabbed and the virus transferred to 2 mL new viral transport buffer, and the 150 mL viral transport reservoir buffer was concentrated to 2 mL using Centricon Plus-70 (Millipore, USA) the same day. After addition of antibiotics, both samples were stored at -80°C until processing with qPCR or viral culture for determination of respiratory virus concentration and infectivity.

Nose and throat swab samples were subjected to in vitro diagnostic-use viral panel, xTAG Respiratory Viral Panel (Abbott Molecular, Illinois, USA), to detect qualitatively 12 common respiratory viruses and subtypes including influenza A (non-specific, H1, and H3) and B, respiratory syncytial virus (RSV, subtypes A and B), parainfluenza (types 1-3), adenovirus, metapneumovirus, coronavirus, and rhinovirus. The xTAG Respiratory Viral Panel has been shown to detect common respiratory viral targets with high sensitivity (100%) and specificity (91%) than other similar panels in over 200 respiratory specimens from adult patients with signs of respiratory infection. After one or more of the candidate respiratory viruses was detected in the nose and throat swab by the Viral Panel, the nose and throat swab, and the exhaled droplets from subjects captured on the impactor plate or the reservoir buffer ($\geq 5\text{ }\mu\text{m}$ or $< 5\text{ }\mu\text{m}$) would be processed with qPCR (and viral culture when a susceptible cell line was available) specific to the candidate virus for determination of virus concentration in different size fractions of aerosols.

The primary outcome of the study was the virus generation rate in the tidal breathing of patients infected by different respiratory viruses, and the efficacy of face mask in preventing virus dissemination. The secondary outcome was the correlation between viral loads in nose/throat swabs and exhaled breath particles. We stratified all analyses by type of respiratory virus infection as determined in the viral panel on the nose swab. We tabulated the respiratory virus positive proportion as determined

by PCR in nasal swabs, throat swabs, exhaled breath coarse particles, and exhaled breath fine particles for the corresponding respiratory virus as identified by the viral panel, among participants who have provided an exhaled breath sample without wearing a face mask stratified by two age groups. For the three groups of respiratory viruses with highest frequency of infection, we plotted log viral load of nasal swab, throat swab, fine/coarse fraction of exhaled breath against age, days since acute respiratory illness onset and mask intervention, number of coughs/sneezes. We investigated the correlations between viral shedding in nose swab, throat swab, fine and coarse fractions of exhaled breath by scatterplot between any two types of samples. We then compared the number of exhaled breath samples containing detectable viral load between patients wearing face mask or not, and tested for significant difference whenever possible by Fisher's exact tests.

Results

From April 2014 to March 2016, of 1746 patients screened, 703 (40%) were eligible and 219 (31%) were recruited. Seven (3%) patients withdrew and the remaining 212 (97%) patients were proceeded to the randomisation of mask intervention for the first exhaled breath collection, and voluntarily provided a second exhaled breath sample of alternate mask intervention. A total of 105 patients were randomised to not wearing a face mask during the first exhaled breath collection and 107 patients randomised to wearing a face mask. To increase the power of the analysis for individual respiratory viruses, we decided to include in the analysis exhaled breath samples collected from 44 patients recruited from a similar study conducted earlier from January 2013 to March 2014. Therefore, in final analysis, 256 patients were included, contributing to 151 exhaled breath samples collected without wearing a face mask and 152 exhaled breath samples collected with wearing a face mask.

Most of the 256 patients were between 18 and 50 years old (77%) and were recruited within 2 days since symptom onset (79%). Infection by at least one of the respiratory viruses included in the viral panel was identified in 153 (60%) of all patients. Infection by enterovirus/rhinovirus was most frequent (n=65, 25%), followed by influenza viruses (n=48, 19%) and human coronaviruses (n=24, 9%).

Four (80%) of five patients aged 11 to 17 years tested positive by the viral panel, including enterovirus/rhinovirus (n=1), influenza A virus (n=2), and influenza B virus (n=1). The respiratory virus infection was confirmed by RT-PCR in nose swabs in the two patients infected with influenza A virus but not in patients infected by other respiratory viruses. For all four patients, none had respiratory viral RNA recovered in their throat swabs or from the coarse or

TABLE. Efficacy of surgical face masks in reducing respiratory virus dissemination

Virus type	No of PCR+ exhaled breath samples					
	Fine particles ≤5 μm			Coarse particles >5 μm		
	Mask	Control	P value	Mask	Control	P value
Enterovirus/rhinovirus	0/25	0/33	-	0/25	0/33	-
Influenza A virus	3/15	6/17	0.44	0/15	4/17	0.10
Influenza B virus	1/9	1/4	1.00	0/9	1/4	0.31
Human coronavirus (NL63, OC43, HKU1)	0/16	1/12	0.43	0/16	0/12	-
Parainfluenza virus (P1, P2, P3, P4)	0/6	0/5	-	0/6	0/5	-
Respiratory syncytial virus	0/2	1/4	1.00	0/2	0/4	-
Human metapneumovirus	1/1	1/2	1.00	0/1	0/2	-

fine particles of the exhaled breath. In addition, 79 (66%) of 119 patients aged ≥18 years tested positive by the viral panel, including enterovirus/rhinovirus (n=33, 27%), influenza A virus (n=16, 13%), influenza B virus (n=3, 3%), and human coronaviruses (n=12, 10%). The respiratory virus infection was confirmed by RT-PCR in nose swabs in patients infected with enterovirus/rhinovirus (30%), influenza A (94%) and B (33%) viruses, and human coronaviruses (17%). Together with other respiratory viruses, we detected among the 153 patients respiratory viral RNA by RT-PCR in 20 (10%) of 152 exhaled breath samples, in the fine fraction in control group (10/77, 13%) and in mask group (5/75, 7%), and in the coarse fraction in control group (5/77, 6%) and in mask group (0/75, 0%).

We selected influenza A, enterovirus/rhinovirus, and human coronavirus for further analysis given the relatively larger sample sizes. We could not detect a significant difference on the effect of surgical masks on viral shedding of influenza A virus in the coarse (P=0.10) and fine (P=0.44) fraction of exhaled breath; nor that of human coronavirus in the fine fraction (P=0.43) [Table].

Discussion

Surgical face masks are inexpensive and easily accessible and are therefore widely used during epidemics of respiratory infections, both as a source control measure in ill persons and as a preventative measure against infection.

Viral RNA was observed in nose/throat swab and in exhaled breath regardless of the number of cough/sneezes produced during collection. We detected influenza A virus and human coronaviruses viral shedding in the fine fraction of exhaled breath from patients with as little as two coughs, and in the coarse fraction in one influenza-infected patient who never coughed, demonstrating that patient could shed virus through exhaled breath to the environment with limited or even without coughing

in both fine and coarse fractions of exhaled breath.

Human rhinovirus, RSV, and adenovirus have been detected in three exhaled breath samples from adults with mild to severe asthma.¹ Among asthmatic children with human rhinovirus infection, 11.5% of virus was detected in exhaled breath samples (compared to 25.5% in nasal wash samples) and one sample had co-infection with non-human rhinovirus.² Viral RNA has been detected from human rhinovirus (45%) and parainfluenza virus (26%) from exhaled breath. Among the patients (29/53) with positive human rhinovirus viral RNA in exhaled breath, they also observed 1 to 3 cases of concurrent detection of parainfluenza virus type 1 and 3, and influenza A virus.

The major limitation of our study was the large proportion of influenza-confirmed patients with undetectable viral shedding in exhaled breath samples. We could have increased the sampling duration beyond 30 minutes to increase the viral load being captured, at the cost of acceptability in some participants. An alternative approach is to invite patients to perform forced coughs during exhaled breath collection.³ However, many of our patients did not cough much or at all, and in our present study we focused on recovering respiratory virus in exhaled breath in a real-life situation. We found that surgical masks were effective in preventing virus dissemination in coarse fraction of exhaled breath even when a participant coughed many times.

Funding

This study was supported by the Health and Medical Research Fund, Food and Health Bureau, Hong Kong SAR Government (#13120592). The full report is available from the Health and Medical Research Fund website (<https://rfs1.fhb.gov.hk/index.html>).

Disclosure

The results of this research have been previously published in:

(1) Leung NHL, Chu DKW, Shiu EYC, et al. Respiratory virus shedding in exhaled breath and efficacy of face masks. *Nat Med* 2020;26:676-80.

References

1. Turchiarelli V, Schinkel J, Molenkamp R, et al. Repeated virus identification in the airways of patients with mild and severe asthma during prospective follow-up. *Allergy* 2011;66:1099-106.
2. Tovey ER, Stelzer-Braid S, Toelle BG, et al. Rhinoviruses significantly affect day-to-day respiratory symptoms of children with asthma. *J Allergy Clin Immunol* 2015;135:663-9.e12.
3. Milton DK, Fabian MP, Cowling BJ, Grantham ML, McDevitt JJ. Influenza virus aerosols in human exhaled breath: particle size, culturability, and effect of surgical masks. *PLoS Pathog* 2013;9:e1003205.

Human parechovirus infection in Hong Kong neonates, infants, and young children: abridged secondary publication

PKS Chan *, MCW Chan, EAS Nelson, TF Leung

KEY MESSAGES

1. Human parechovirus (HPeV) infection occurred in about 2.3% of all young children (≤ 3 months) hospitalised for acute viral illnesses.
2. HPeV infection exhibited a distinct seasonality, with most infections occurring in September to January (autumn and winter).
3. The more pathogenic type, HPeV3, was rare in Hong Kong.
4. Clinical presentation of HPeV ranged from mild gastroenteritis, upper respiratory tract infection, and febrile rash to convulsion and severe sepsis.

5. Diagnostic service for HPeV should be made available for young infants presenting with sepsis.

Hong Kong Med J 2020;26(Suppl 4):S8-11
HMRP project number: 13120362

¹ PKS Chan, ¹ MCW Chan, ² EAS Nelson, ² TF Leung

¹ Department of Microbiology, The Chinese University of Hong Kong, Hong Kong

² Department of Paediatrics, Prince of Wales Hospital, Hong Kong

* Principal applicant and corresponding author: paulkschan@cuhk.edu.hk

Introduction

There are 16 types of human parechovirus (HPeV), which is fastidious to grow and can escape detection by polymerase chain reaction (PCR) based on pan-enterovirus primers. Most laboratories do not offer testing for HPeV, and therefore many epidemiological and clinical aspects of this virus remain unknown.

Currently available data indicate that HPeV1 is the most common type found and is associated with mild gastrointestinal illnesses. HPeV3 is more often associated with severe diseases (including sepsis and meningoencephalitis), especially in neonates.¹

Methods

This 24-month prospective study was conducted at the Prince of Wales Hospital in Hong Kong that has a catchment population of about 650 000 including about 25 000 children under 5 years old. During the study period, children aged ≤ 36 months who were admitted to the hospital for suspected acute viral illnesses were identified. A targeted number of patients from each age group were randomly selected for study every week. Specimens were tested for HPeV, in addition to the routine virological and bacteriological investigations. This study was approved by the Joint Chinese University of Hong Kong – New Territories East Clinical Research Ethics Committee.

HPeV RNA was detected by real-time PCR,² and genotype was assigned based on the maximum likelihood tree topology constructed using RAXML MPI v8.2.8 based on the global nucleotide alignment of the VP1 gene sequences. The distribution in

HPeV types observed in this study was compared to that reported worldwide by the weighted GUniFrac method.

Children with symptoms of acute gastroenteritis were tested for rotavirus and norovirus on a routine basis. Stool samples positive for HPeV were subjected to multiplex PCR, which is capable of detecting viruses associated with acute gastroenteritis, including rotavirus, norovirus, adenovirus 40/41, sapovirus, astrovirus, and aichi virus.

Results

A total of 3911 children were recruited between March 2014 and February 2016, with 129 to 225 examined per month. The male-to-female ratio was 1.3:1, and 7.3% were neonate, 37.0% were 4 weeks to 12 months, 30.4% were 13 to 24 months, and 25.4% were 25 to 36 months.

A total of 4567 specimens collected from the 3911 children were tested for HPeV: 58.0% were nasopharyngeal aspirate (NPA) samples; 32.5% were stool samples or rectal swabs; 4.4% were cerebrospinal fluid; and 5.0% were blood and other miscellaneous samples.

Of the 3911 children, 49 boys and 39 girls were detected to have HPeV. Of them, 3 (3.4%) were neonates, 40 (45.5%) were aged 4 weeks to 12 months, 29 (33.0%) were aged 13 to 24 months, and 16 (18.2%) were aged 25 to 36 months.

A sharp seasonality was observed with 87.5% (77/88) of infections detected between September and January, corresponding to the autumn and

winter seasons in Hong Kong (Fig 1). The same seasonal pattern was observed in both years.

Of the 88 children infected with HPeV, 80 (90.9%) had samples with virus type identified. In both seasons, HPeV1 predominated and accounted for 81.3% (65/80) of infections, followed by HPeV4 (12.5%, 10/80). Other HPeV types were rare: HPeV3 (n=2), HPeV6 (n=2), and HPeV5 (n=1).

The distribution pattern of virus type of the 88 children was compared with that of 20 studies, including one from Hong Kong. The distribution pattern of HPeV types could be broadly divided into three groups based on clustering analysis using the weighted GUniFrac method. The pattern of Hong Kong was close to that reported from Guangzhou (China), Lanzhou (China), and Thailand where HPeV1 predominated with a small number of HPeV3/4. In contrast, HPeV3 predominated in studies from Japan, Denmark, Spain, France, and United Kingdom. The Netherlands, Italy, Taiwan, Japan, and China have reported a co-circulation of both HPeV1 and HPeV3 types.

Children with HPeV1 infection were significantly older than those with non-HPeV1 infection (12 [9-19] months vs 7 [6-17.5] months, P=0.450).

Regarding clinical presentation, when HPeV was the only infection identified, it was regarded as having a 'probable' association with the illness. When HPeV was detected in association with other conventional pathogens of the illness, the role of HPeV was regarded as 'uncertain'. Because the association between respiratory and gastrointestinal pathogens with neurological presentation is less clear, the role of HPeV was regarded as 'suspected' in these cases (Fig 2).

For acute gastroenteritis, 27 (30.7%) of the 88 infected children were regarded as having HPeV being a 'probable' cause. Among them, 25 (92.6%) had diarrhoeal symptoms, with the frequency varying from once a day to >10 times a day. In contrast, only 12 (44.4%) of 27 children had vomiting, which was usually mild. Four children also had HPeV detected from NPA, with two of them being coinfecting with parainfluenza type 2 or respiratory syncytial virus and all having respiratory symptoms. In addition, 30 (37.5%) of the 88 infected children had symptoms of acute gastroenteritis and HPeV detected from stool, but the role of HPeV was regarded as 'uncertain', because other gastroenteritis-associated pathogens (most commonly norovirus, rotavirus, *Salmonella* and *Campylobacter spp*) were also found in stool samples. Four of the 30 children also developed rash.

For acute respiratory illness, 11 (12.5%) of the 88 HPeV-infected children were regarded as having HPeV being a 'probable' cause. The most common symptoms were cough and runny nose. Five children had mild shortness of breath or noisy breathing, and

one developed pneumonia with chest X-ray showing mild left perihilar haziness but without significant consolidation. Six (54.5%) of the 11 children also had HPeV detected from stool. Five children also developed symptoms of acute gastroenteritis, with two having coinfection with *Salmonella enteritidis* or *Campylobacter jejuni*. In addition, 20 children with HPeV detected from NPA also had coinfection with other respiratory pathogens; 12 (60.0%) of them developed lower respiratory tract involvement with acute bronchiolitis or pneumonia.

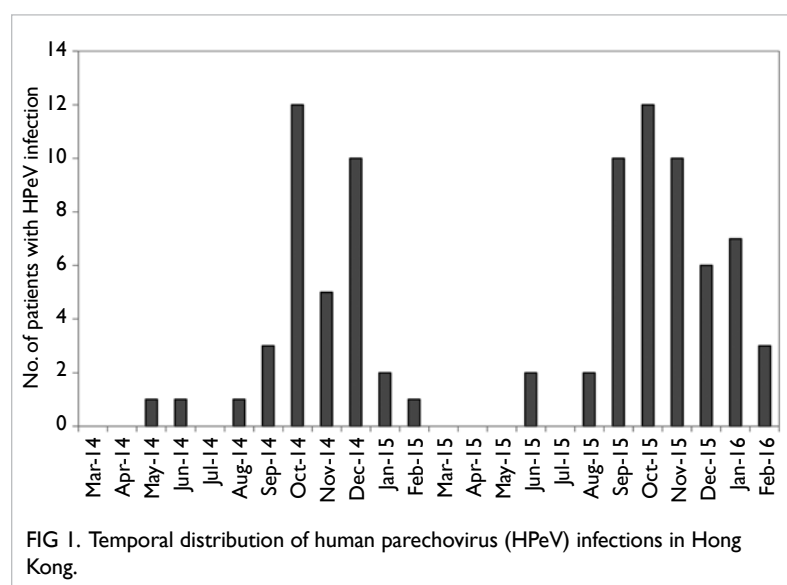


FIG 1. Temporal distribution of human parechovirus (HPeV) infections in Hong Kong.

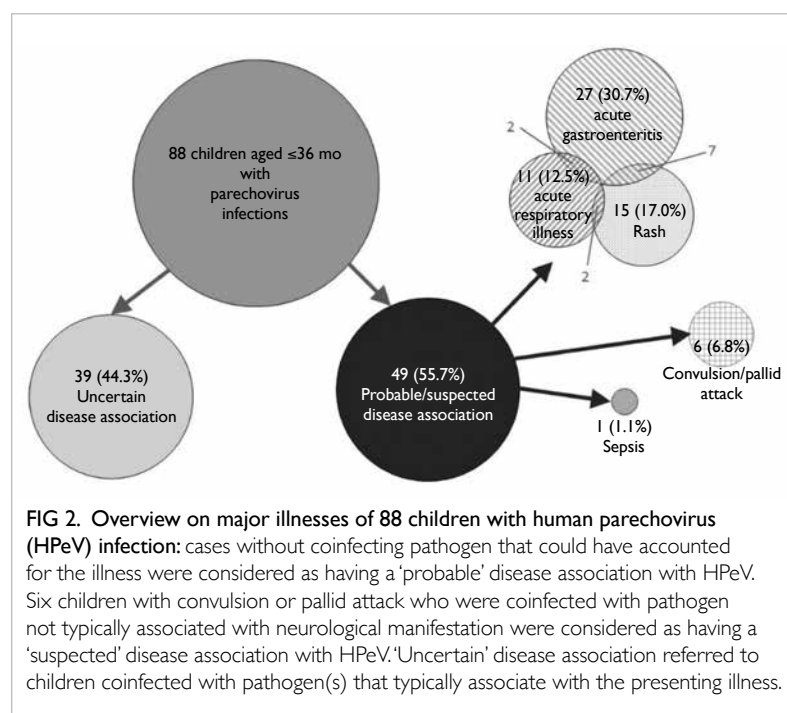


FIG 2. Overview on major illnesses of 88 children with human parechovirus (HPeV) infection: cases without coinfecting pathogen that could have accounted for the illness were considered as having a 'probable' disease association with HPeV. Six children with convulsion or pallid attack who were coinfecting with pathogen not typically associated with neurological manifestation were considered as having a 'suspected' disease association with HPeV. 'Uncertain' disease association referred to children coinfecting with pathogen(s) that typically associate with the presenting illness.

TABLE I. Characteristics of human parechovirus (HPeV)-infected children with rash illness

Case No.	Sex/ age, m	Presentation of rash	Concurrent illness(es)	Sample(s) positive for HPeV	HPeV type	Coinfections
16	M/30	Itchy blanchable maculopapular rash over back, spread to trunk, forearms, and feet.	Acute gastroenteritis	Stool	HPeV1	Rhinovirus and non-typhoidal <i>Salmonella spp</i>
24	M/7	Mild fine blanchable maculopapular rash over face, trunk, and right scrotum, sparing limbs. Developed after fever subsided. Clinically considered as roseola.	Acute gastroenteritis, upper respiratory tract illness	Stool	HPeV4	-
27	F/9	Maculopapular rash over face and body. Developed after fever subsided. Clinically considered as roseola.	Acute gastroenteritis, upper respiratory tract illness	Stool	HPeV1	-
34	F/19	Maculopapular rash over buttock and hands, with fever for 3 days.	Acute gastroenteritis, upper respiratory tract illness	Stool	HPeV1	Parainfluenza virus type 1
43	M/6	A few spots of rash over back, face, and neck, with fever for 9 days.	Acute gastroenteritis, upper respiratory tract illness	Stool	HPeV4	Rhinovirus, non-typhoidal <i>Salmonella spp</i>
49	M/10	Generalised whole body maculopapular rash, with fever for 2 days.	Acute gastroenteritis, upper respiratory tract illness	Stool	HPeV1	-
50	M/16	Maculopapular rash over trunk after fever subsided. Clinically considered as roseola.	Acute gastroenteritis	Stool	Typing failed	-
51	F/3	Eczematous rash over chest, with fever.	Acute gastroenteritis, bronchiolitis	Stool	HPeV1	Respiratory syncytial virus
57	F/20	Blanchable macular rash over forehead, erythematous periorbital swelling, with fever.	Upper respiratory tract illness	Stool, blood	HPeV4	-
58	M/11	Generalised maculopapular rash. Developed after fever subsided. Clinically considered as roseola.	Upper respiratory tract illness	Stool, nasopharyngeal aspirate	HPeV1	-
67	F/20	Itchy rash over trunk and spread to limbs and scalp, weeping, crusting, peeling, and sandpaper-like. Features of cellulitis. No fever.	-	Rectal swab	HPeV4	<i>Staphylococcus aureus</i> from skin swab
68	M/8	Eczematous rash, with fever.	Acute gastroenteritis, croup, pneumonia	Stool	HPeV4	-
76	F/7	A few patches of maculopapular rash over right hand only, no fever.	Acute gastroenteritis, upper respiratory tract illness	Stool	HPeV4	Norovirus, rhinovirus
77	F/7	On and off skin rash, faint scattered spots over face and trunk.	Acute gastroenteritis	Stool, nasopharyngeal aspirate	HPeV1	Norovirus
81	M/16	Mild generalised erythematous patches, with fever.	Bronchiolitis	Nasopharyngeal aspirate	HPeV1	-
87	M/10	Maculopapular rash over trunk. Developed after fever subsided. Clinically considered as roseola.	Upper respiratory tract illness	Stool, nasopharyngeal aspirate	HPeV1	Parainfluenza type 1

For rash, 15 (17.1%) of 88 children were regarded as having HPeV being a 'probable' cause. In all except one child, HPeV was found from stool/rectal swab (Table). The rash presentation was mainly maculopapular and often generalised involving trunk and limbs, and accompanied with fever or developed just after fever had subsided. Most of these children presented with other concurrent illnesses such as acute gastroenteritis and mild upper respiratory tract illness. A 20-month-old girl developed an itchy, weeping, crusting, sand paper-like rash on the scalp and limbs, without fever. The skin swab was positive

for *Staphylococcus aureus*. The HPeV4 found in the stool of this child was likely to be a bystander.

Six (6.8%) of the 88 HPeV-infected children developed neurological illnesses, including convulsion (n=5) and pallid attack (n=1). All these children had concurrent illnesses that could be explained by the coinfection identified. Three children had acute gastroenteritis secondary to norovirus or non-typhoidal *Salmonella spp*. Another three children had upper respiratory tract infections with rhinovirus or parainfluenza type 3 virus. Because association between HPeV and coinfecting

pathogens and the neurological presentation could not be verified in these children, HPeV was regarded as a 'suspected' pathogen.

Only one child presented with sepsis. A 6-day-old female neonate born full term by vaginal delivery presented with fever up to 38.6°C, with no respiratory or gastrointestinal symptoms. Her heart rate was 200 beats per min. She was given an intravenous bolus of normal saline of 40 mL/kg body weight but tachycardia and metabolic acidosis persisted despite blood pressure being maintained in the normal range. She was empirically treated with intravenous ampicillin and amikacin. Her infection markers including white cell count and C-reactive protein were not raised, despite presentation of impending shock. Ultrasonographic examination of abdomen was unremarkable. Blood, urine, and cerebrospinal fluid cultures were all negative. Chest X-ray showed only mild bilateral lung field streakiness. Her NPA was positive for HPeV3, which was the only pathogen identified.

The six children presenting with neurological illness in which HPeV was regarded as a 'suspected' cause were significantly older than other children who presented with acute gastroenteritis (25 [22.5-29.0] months vs 11.0 [7-15.5] months, $P < 0.01$), acute respiratory illness (25 [22.5-29.0] months vs 13.0 [10.5-18.5] months, $P < 0.01$), and rash (25 [22.5-29.0] months vs 10.0 [7-16] months, $P < 0.01$).

Discussion

The distribution pattern of virus type of the 88 children was very similar to that reported from Guangzhou where travel of people is very frequent.³ In contrast, HPeV3 was rarely detected in Hong Kong (2/80, 2.5%), although it is commonly found in Europe and a few Asian cities. This may have implications on local disease burden, as HPeV1 is more likely to be associated with mild gastroenteritis, and HPeV3 is more likely to be associated with severe diseases (including sepsis, meningoencephalitis, and myocarditis) in infants below the age of 3 months.⁴

In Hong Kong, the prevalence of HPeV4 is relatively high, which is also seen in nearby cities. HPeV4 occurred more frequently in children with rash illness. A characteristic pattern of rash with palmar-plantar distribution has been described in young infants infected with HPeV3.⁵ However, the presentation of rash illness associated with other HPeV types, or in older infants and young children is less well defined. In the current study, most children who developed a generalised maculopapular rash

mainly involved face and limbs and accompanied with fever.

We suspect coinfection of HPeV with other respiratory viruses may confer a higher chance of low respiratory tract involvement, as 60% of these children had acute bronchiolitis or pneumonia.

Conclusions

HPeV infection had a clear seasonality in Hong Kong and was found in 2.3% of all children aged ≤ 36 months hospitalised for suspected acute viral illnesses. In about half of the cases, HPeV probably contributed to the disease, most commonly acute mild acute gastroenteritis, upper respiratory tract infection, and generalised maculopapular rash. Sepsis was found in a neonate. Further study is warranted to clarify the role of HPeV in causing convulsion and aggravating other respiratory viral infections. Diagnostic service for HPeV should be made available for young infants presenting with sepsis.

Funding

This study was supported by the Health and Medical Research Fund, Food and Health Bureau, Hong Kong SAR (#13120362). The full report is available from the Health and Medical Research Fund website (<https://rfs1.fhb.gov.hk/index.html>).

Disclosure

The results of this research have been previously published in:

(1) Chiang GPK, Chen Z, Chan MCW, et al. Clinical features and seasonality of parechovirus infection in an Asian subtropical city, Hong Kong. *PLoS One* 2017;12:e0184533.

References

1. de Crom SC, Rossen JW, van Furth AM, Obihara CC. Enterovirus and parechovirus infection in children: a brief overview. *Eur J Pediatr* 2016;175:1023-9.
2. Nix WA, Maher K, Johansson ES, et al. Detection of all known parechoviruses by real-time PCR. *J Clin Microbiol* 2008;46:2519-24.
3. Chen H, Yao Y, Liu X, et al. Molecular detection of human parechovirus in children with acute gastroenteritis in Guangzhou, China. *Arch Virol* 2014;159:971-7.
4. van der Sanden S, de Bruin E, Vennema H, Swanink C, Koopmans M, van der Avoort H. Prevalence of human parechovirus in the Netherlands in 2000 to 2007. *J Clin Microbiol* 2008;46:2884-9.
5. Shoji K, Komuro H, Kobayashi Y, et al. An infant with human parechovirus type 3 infection with a distinctive rash on the extremities. *Pediatr Dermatol* 2014;31:258-9.

Effect of increased influenza and pneumococcal vaccine coverage on the burden of influenza among elderly people in Hong Kong versus Brisbane: abridged secondary publication

L Yang *, WB Hu, CM Wong, SSS Chiu, RJ Soares Magalhaes, TQ Thach, ACA Clements, JSM Peiris

KEY MESSAGES

1. Influenza and pneumococcal vaccine uptake in older adults of Hong Kong has dramatically increased since the SARS outbreak in 2003. This enables estimation of the effect of increased vaccine coverage by comparing the relative change in influenza disease burden with Brisbane, where vaccine coverage remained stable before and after 2003.
2. Compared with the low vaccination period (pre-SARS), during the first 6 years of high vaccination (post-SARS), influenza-associated excess rates of cardio-respiratory disease, stroke, and ischaemic heart diseases mortality decreased more in Hong Kong than in Brisbane.
3. After the 2009 H1N1 pandemic, excess rates of all-causes mortality increased in Hong Kong but to a lesser extent than in Brisbane.
4. This study provides limited evidence that

markedly increased vaccination rates have reduced influenza disease burden in elderly people of Hong Kong.

Hong Kong Med J 2020;26(Suppl 4):S12-6
HMRF project number: 13121282

¹ L Yang, ² WB Hu, ³ CM Wong, ⁴ SSS Chiu, ⁵ RJ Soares Magalhaes, ⁶ TQ Thach, ⁶ ACA Clements, ³ JSM Peiris

¹ School of Nursing, The Hong Kong Polytechnic University, Hong Kong

² School of Public Health and Social Work, Queensland University of Technology, Australia

³ School of Public Health, The University of Hong Kong, Hong Kong

⁴ Department of Paediatrics and Adolescent Medicine, The University of Hong Kong, Hong Kong

⁵ School of Veterinary Science, University of Queensland, Australia

⁶ Research School of Population Health, Australian National University, Australia

* Principal applicant and corresponding author: l.yang@polyu.edu.hk

Introduction

Influenza is associated with heavy burden of mortality and morbidity globally. Vaccination is an important strategy to reduce disease severity and virus transmission within the community. Few studies have been conducted in high-risk older peoples or those with underlying chronic conditions, although many countries recommend annual influenza vaccination or subsidy programmes to these high-risk groups. An ongoing debate on the true effectiveness of influenza vaccines in the elderly people highlights a need to evaluate the impact of influenza vaccines at the population level.¹

In Hong Kong, the annual vaccination rate for community-dwelling elders were <3% between 2000 and 2002,² but it increased to >50% between 2004 and 2006.³ In Australia, free influenza vaccine is provided for people aged ≥65 years since 1999, and the coverage rate in older adults was 70% to 80% between 2002 and 2006.⁴ Unlike Hong Kong, where the SARS outbreak and new subsidy programme greatly increased the influenza and pneumococcal vaccine coverage in the elders, Brisbane has a fairly stable vaccination rate since 2000.

We compared the long-term trend of influenza burden in those aged ≥65 years in Hong Kong and Brisbane, with the aim to quantify the impact of influenza and pneumococcal vaccine coverage on the reduction of influenza disease burden. Given the similar socioeconomic and climate conditions between the two cities, we hypothesise that the dramatically increased uptake of influenza vaccine among elderly people of Hong Kong since SARS should have reduced mortality and hospitalisation associated with influenza in a larger extent than that in Brisbane where the vaccine uptake remained stable.

Methods

Weekly numbers of specimens tested positive for influenza A and B and weekly total numbers of specimens collected in Hong Kong were obtained from the microbiology laboratory of Queen Mary Hospital. In addition, weekly positive numbers of influenza A and B of Brisbane during 30 April 2001 to 1 January 2010 were obtained from the Queensland Health Australia, but virology data afterwards were not available. Therefore, virology

data of the Queensland state during 2 January 2010 to 16 December 2012 were obtained to approximate the virus activity in Brisbane.

Death registry data were obtained from the Census and Statistics Department of Hong Kong and from Australian Institute of Health and Welfare. Mortality data were aggregated into weekly numbers of deaths with underlying causes of all-causes (ICD10 A00-T99), cardio-respiratory disease (CRD) [ICD10 I00-J99], pneumonia and influenza (P&I) [ICD10 J09-J18], chronic obstructive pulmonary disease (COPD) [ICD10 J40-J47], stroke (ICD9 430-438; ICD10 I60-I69), and ischaemic heart diseases (IHD) [ICD10 I20-I25].

Hospital admission data were obtained from the Hospital Authority of Hong Kong and Queensland Health Australia. Weekly numbers of hospital admissions were aggregated by the discharge diagnosis of CRD (ICD9 390-459), acute respiratory disease (ICD9 460-519), P&I (ICD9 480-487), COPD (ICD9 490-496), stroke (ICD9 001-999), and IHD (ICD9 410-414).

Meteorology data including daily mean of temperature and relative humidity from 2001 to 2013 were obtained from the Hong Kong Observatory and

Australian Bureau of Meteorology.

In Hong Kong, seasonal influenza peaks during January to March and June to July, whereas in Australia the influenza peaks during August to October (Fig). Given the difference in seasonal influenza peaks in these two cities, we define the influenza season as January to December in Hong Kong and May to April in Brisbane. The start dates of these seasons are three months after the usual launch dates of the annual seasonal influenza vaccination campaign (March in Brisbane and September in Hong Kong). This should allow valid assessment of the impact of vaccination. The periods defined for influenza associated disease burden estimates in Hong Kong and Brisbane are listed in Table 1.

We constructed time series segmented regression models to estimate mortality or hospitalisation risks associated with influenza in elderly people during the pre-SARS, post-SARS, and post-pandemic period for Hong Kong and Brisbane. The proxy variable of influenza in the model is the percentage of specimens positive for influenza each week among the annual total number of positive specimens in each city. The confounders of seasonal trend, temperature, humidity, and other respiratory

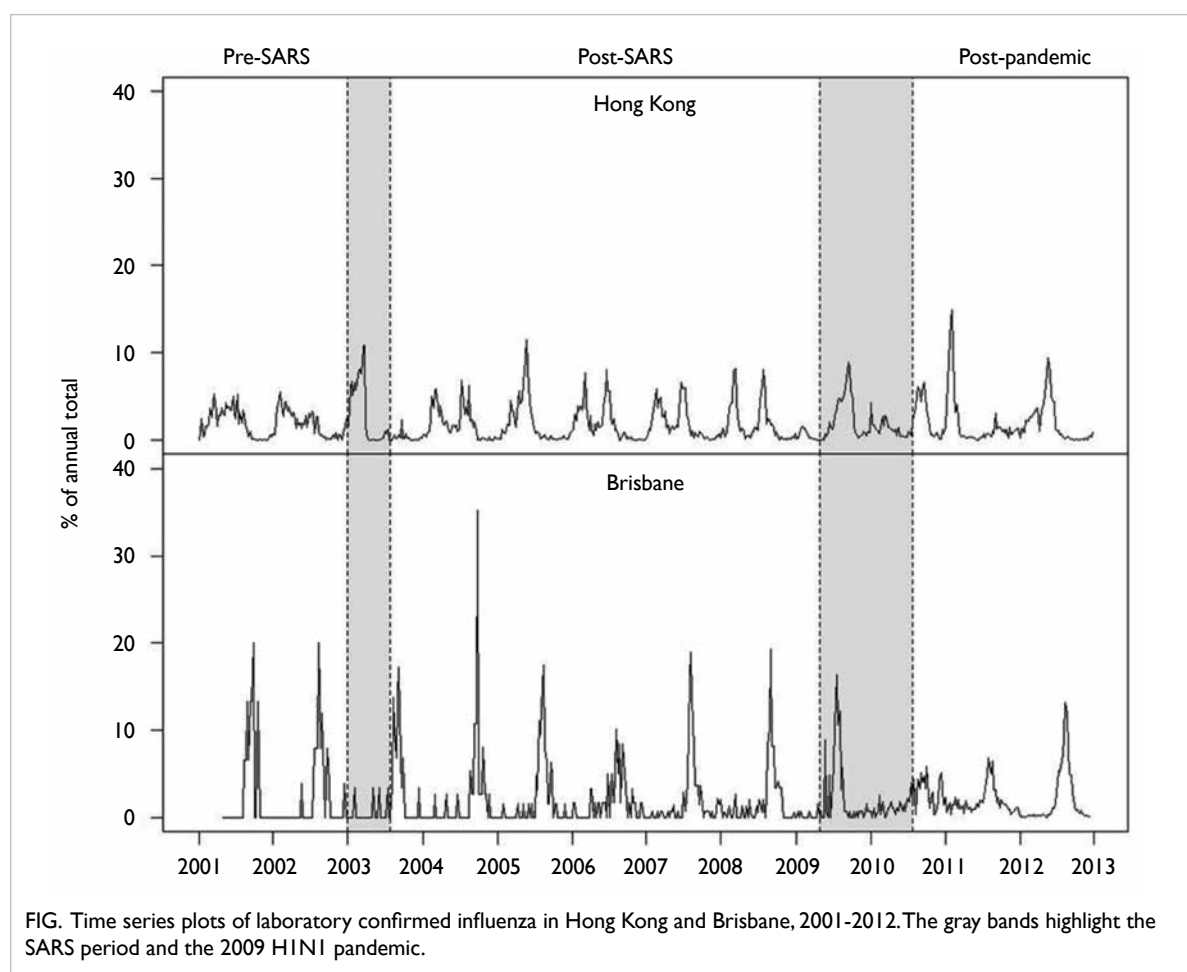


FIG. Time series plots of laboratory confirmed influenza in Hong Kong and Brisbane, 2001-2012. The gray bands highlight the SARS period and the 2009 H1N1 pandemic.

TABLE 1. Study periods defined for Hong Kong and Brisbane

Period	Hong Kong			Brisbane		
	Start date	End date	No of weeks	Start date	End date	No of weeks
Pre-SARS	31/12/2000	29/12/2002	104	30/04/2001	29/12/2002	87
SARS	30/12/2002	02/08/2003	31	30/12/2002	03/08/2003	31
Post-SARS	03/08/2003	25/04/2009	299	04/08/2003	26/04/2009	299
Pandemic	26/04/2009	31/07/2010	66	27/04/2009	01/08/2010	66
Post-pandemic	01/08/2010	29/12/2012	126	02/08/2010	16/12/2012	124

viruses were added into the model to assess influenza-associated excess risk. Dummy variables for the pre-SARS, post-SARS, and post-pandemic periods, together with the interaction terms between these period dummies and virus activity variables, were also added to test the statistical difference in the risk estimates between the different periods within each city. Baseline rates of cause-specific mortality and hospitalisation associated with influenza were calculated for different periods by setting the virus proxy to zero and the corresponding period dummy to one (other dummies set to zero simultaneously). Excess numbers were derived by subtracting baseline rates from observed data, and excess rates were further calculated by dividing age-specific population size. The 95% confidence interval of the excess rate was calculated by bootstrapping for 1000 times. Due to the different length of periods, we calculated annual rates of excess mortality (or hospitalisation) to facilitate the comparison between different periods.

The pre-SARS period was the reference period. For each disease category, the rate ratio (RR) of post-SARS (or post-pandemic) versus pre-SARS was derived by dividing the annual excess rates during the post-SARS (or post-pandemic) period to those in the pre-SARS period: $RR = \text{annual excess rate (post-SARS)} / \text{annual excess rate (pre-SARS)}$. The ratio of RR (RRR) was calculated by dividing RR of Hong Kong with RR of Brisbane. We used the ratio of RR as measurement of relative change in influenza disease burden, because the ratio of RR is less likely to be affected by the regional heterogeneity of these factors between Hong Kong and Brisbane, compared to the commonly adopted excess mortality/hospitalisation. The 95% confidence interval and P value of RR and RRR were derived from normal approximation of their logarithm transformations. All analyses were conducted in R software version 2.5.1. Significance level was set to 0.05.

Results

Compared with the pre-SARS period, the post-SARS period had increased influenza-associated mortality

rates in terms of all-causes (RR=1.22) and COPD (RR=1.04). In Brisbane, all-causes mortality reduced (RR=0.87) and COPD mortality increased but to a slightly less extent than in Hong Kong (RR=1.03, RRR=1.01, P=0.98) [Table 2]. Decreased excess rates of mortality in Hong Kong were observed for CRD (RR=0.90), stroke (RR=0.74), and IHD (RR=0.45) mortality; the corresponding RRs in Brisbane were 0.79, 0.33, and 1.09, respectively. Only IHD mortality shows a significantly greater reduction in Hong Kong than in Brisbane (RRR=0.41, P=0.005).

Compared with the pre-SARS period, in the post-SARS period, excess rates of CRD hospitalisation decreased in Hong Kong but markedly increased in Brisbane (RR=0.86 vs RR=26.82, RRR=0.03, P<0.001). Influenza-associated hospitalisation of P&I and COPD increased more in Brisbane (RR=3.49 and RR=1.33, respectively) than in Hong Kong (RR=2.79 and RR=1.04, respectively), but the differences were not significant (RRR=0.80 and RRR=0.79, respectively). However, the extremely large point estimate for the RR of CRD hospitalisation in Brisbane is due to the very small point estimate of excess CRD hospitalisation rate for the pre-SARS period, which requires a cautious interpretation.

Compared with the pre-SARS period, in the post-SARS period, the excess mortality rates increased in Hong Kong for all the disease categories except IHD, but only all-causes and COPD mortality also increased in Brisbane. The differences between Hong Kong and Brisbane were significant for all-causes and stroke mortality. Annual excess rates of all-causes mortality increased in Hong Kong to a lesser extent than in Brisbane (RR=1.41 vs RR=2.39, RRR=0.59, P<0.001), whereas an opposite changing trend was observed for stroke mortality (RR=1.26 vs RR=0.29, RRR=4.37, P=0.003).

Due to the negative estimates in annual excess rates of mortality, the post-SARS RR could not be estimated for IHD hospitalisation of Hong Kong, P&I mortality, stroke and IHD hospitalisation of Brisbane. Similarly, the post-pandemic RR could not be estimated for P&I and IHD of Hong Kong, and stroke and COPD of Brisbane.

TABLE 2. Rate ratio (RR) for excess mortality or hospitalisation associated with influenza between the post-SARS and pre-SARS (reference) periods and the ratio of RR (RRR) in Hong Kong and Brisbane

	Hong Kong	Brisbane	Hong Kong vs Brisbane	
	RR (95% confidence interval)	RR (95% confidence interval)	RRR (95% confidence interval)	P value (z-test)
Mortality of post-SARS vs pre-SARS				
All-causes	1.22 (1.10-1.35)	0.87 (0.62-1.21)	1.40 (0.99-1.98)	0.058
Cardio-respiratory disease	0.90 (0.80-1.01)	0.79 (0.54-1.15)	1.14 (0.77-1.69)	0.516
Pneumonia and influenza	2.50 (2.00-3.13)	NE	NE	-
Chronic obstructive pulmonary disease	1.04 (0.78-1.38)	1.03 (0.44-2.39)	1.01 (0.41-2.47)	0.980
Stroke	0.74 (0.50-1.09)	0.33 (0.13-0.80)	2.27 (0.85-6.05)	0.102
Ischaemic heart diseases	0.45 (0.34-0.58)	1.09 (0.62-1.90)	0.41 (0.22-0.76)	0.005
Hospitalisation of post-SARS vs pre-SARS				
Cardio-respiratory disease	0.86 (0.82-0.91)	26.82 (9.56-75.24)	0.03 (0.01-0.09)	<0.001
Pneumonia and influenza	2.79 (2.57-3.03)	3.49 (1.96-6.21)	0.80 (0.45-1.43)	0.451
Chronic obstructive pulmonary disease	1.04 (0.96-1.14)	1.33 (0.91-1.93)	0.79 (0.54-1.15)	0.217
Stroke	0.15 (0.12-0.19)	NE	NE	-
Ischaemic heart diseases	NE	NE	NE	-
Mortality of post-pandemic vs pre-SARS				
All-causes	1.41 (1.28-1.56)	2.39 (1.83-3.12)	0.59 (0.44-0.79)	<0.001
Cardio-respiratory disease	1.16 (1.04-1.29)	0.98 (0.69-1.38)	1.19 (0.83-1.71)	0.352
Pneumonia and influenza	2.44 (1.95-3.05)	NE	NE	-
Chronic obstructive pulmonary disease	1.07 (0.81-1.41)	1.75 (0.83-3.67)	0.61 (0.28-1.35)	0.225
Stroke	1.26 (0.90-1.77)	0.29 (0.12-0.72)	4.37 (1.66-11.48)	0.003
Ischaemic heart diseases	0.74 (0.59-0.92)	NE	NE	-

Abbreviation: NE denotes not estimated owing to negative estimates in annual excess rates

Discussion

We estimated the excess rates of mortality or hospitalisation attributable to influenza in pre-SARS, post-SARS, and post-pandemic periods for Hong Kong and Brisbane. We hypothesised that influenza disease burden decreased more or increased less in Hong Kong than in Brisbane since 2003, because the uptake rate of influenza and pneumococcal vaccines was more markedly increased in Hong Kong than in Brisbane at the same time. In a study comparing the relative change in disease burden in Ontario (after a universal influenza vaccination programme was launched) and other Canadian provinces without such a policy.⁵ Influenza-associated mortality reduced in both Ontario and other provinces, but the former had a larger reduction (RRR=0.61).⁵ In the current study, compared with the pre-SARS period, during the post-SARS period, annual excess rates of IHD mortality decreased more in Hong Kong than in Brisbane, but for all the other mortality outcomes, excess rates increased more in Hong Kong (although the differences were not significant). For

hospitalisation in the post-SARS period, significantly reduced excess rates were only found for CRD in Hong Kong. P&I and COPD hospitalisation rates increased in both cities, and the ratio of RRs of Hong Kong versus Brisbane was <1, although none of these estimates were significant.

Conclusion

Our findings provided limited evidence on the effective reduction of influenza-associated disease burden in older adults after the markedly increase of influenza vaccination coverage.

Acknowledgement

We thank the Census and Statistics Department, Hospital Authority of Hong Kong, Hong Kong Observatory, Australian Bureau of Meteorology, Australian Institute of Health and Welfare, Department of Health of the Australian Government, and Queensland Health Australia for providing the datasets.

Funding

This study was supported by the Health and Medical Research Fund, Food and Health Bureau, Hong Kong SAR Government (#13121282). The full report is available from the Health and Medical Research Fund website (<https://rfs1.fhb.gov.hk/index.html>).

Disclosure

Results from this study have been previously published in:

(1) Wang XL, Wong CM, Yang L, et al. Developing an epidemic forecasting model for influenza A in Brisbane, Australia based on climate and Hong Kong influenza A surveillance data. *Clin Infect Dis* 2014;59:1508-9.

(2) Yang L, Chan KP, Wong CM, et al. Comparison of influenza disease burden in older populations of Hong Kong and Brisbane: the impact of influenza and pneumococcal vaccination. *BMC Infect Dis*

2019;19:162.

References

1. Beyer W, McElhaney J, Smith DJ, Monto AS, Nguyen-Van-Tam JS, Osterhaus AD. Cochrane re-arranged: support for policies to vaccinate elderly people against influenza. *Vaccine* 2013;31:6030-3.
2. Hui SL, Chu LW, Peiris JS, Chan KH, Chu D, Tsui W. Immune response to influenza vaccination in community-dwelling Chinese elderly persons. *Vaccine* 2006;24:5371-80.
3. Cowling BJ, Fung RO, Cheng CK, et al. Preliminary findings of a randomized trial of non-pharmaceutical interventions to prevent influenza transmission in households. *PLoS One* 2008;3:e2101.
4. Australian Institute of Health and Welfare. 2002 Influenza Vaccine Survey: Summary results. 2003.
5. Kwong JC, Stukel TA, Lim J, et al. The effect of universal influenza immunization on mortality and health care use. *PLoS Med* 2008;5:e211.

Severity profiles of respiratory viruses in children in Hong Kong: abridged secondary publication

P Wu *, BJ Cowling, JSM Peiris

KEY MESSAGES

1. There was substantial respiratory disease burden associated with influenza, respiratory syncytial virus, parainfluenza, and adenovirus in children in Hong Kong, but virus-attributable deaths were rare.
2. Respiratory disease burden varies in young and old children.
3. Severity of infections with common respiratory viruses can be quantified using data collected

from different sources.

Hong Kong Med J 2020;26(Suppl 4):S17-21
HMRF project number: 13120802

P Wu, BJ Cowling, JSM Peiris

School of Public Health, The University of Hong Kong, Hong Kong

* Principal applicant and corresponding author: pengwu@hku.hk

Introduction

Most respiratory virus infections lead to mild self-limiting illness, but on some occasions infection may lead to severe diseases such as viral pneumonia or secondary bacterial pneumonia. Considerable numbers of respiratory viruses have been detected from outpatients and inpatients with influenza-like illness or other respiratory infections.¹⁻³ Effects of respiratory viruses on population morbidity and mortality have been well studied,⁴ no studies have systematically investigated the impact associated with common respiratory viruses and compared relative contributions from these viruses to disease burden. Therefore, we examined the impact of four common respiratory viruses in Hong Kong. We constructed an impact pyramid for each virus by estimating the number of symptomatic infections, medically attended infections, virus associated excess hospitalisations, intensive care unit (ICU) admissions, and deaths during 2009 and 2012.

Methods

Estimation of symptomatic infections

In 2008 to 2010, we conducted a randomised controlled trial to evaluate the direct and indirect benefits of influenza vaccination for children.^{5,6} In October 2008 we began a pilot study in 119 households and in October 2009 we began a larger main trial in 796 households. One child in each household was randomised to receive influenza vaccination or placebo. Households were followed up for 1 year prospectively to identify illnesses, and nose and throat swabs were collected from ill children. We continued to follow up the subjects without administering any further vaccinations in 2010 to 2011 and 2011 to 2012. Nasal and throat

swabs are routinely collected from symptomatic subjects reporting illness. Specimens collected from unvaccinated children were used in the present proposal to provide information on the incidence of symptomatic infections associated with various respiratory viruses. We tested 600 specimens from unvaccinated children 0-15 years for respiratory syncytial virus, parainfluenza and adenovirus by the xTAG multiplex array that permits testing of multiple respiratory viruses in a single sensitive assay.⁷

Incidence of medically attended infection

To estimate the probability of symptomatic cases seeking medical service, we conducted a population-based survey on patterns of health seeking behaviour among 1000 randomly selected parents with at least one child aged 0 to 15 years. Subjects were selected through household recruitment by random digital dialling of landline numbers. The recruited parents were asked about the intention to take their sick child to seek medical consultation if the child had acute respiratory symptoms, which were regarded as the driving factor for health-seeking behaviour by the parents. The information collected on the proportion of subjects with febrile respiratory infections seeking medical consultation were used to derive the probability of an infection leading to a medical consultation at a private general practitioner, a public general outpatient clinic, or a hospital emergency room for each virus of interest.

Incidence of hospitalisations, ICU admissions, and deaths

Weekly age-specific all-cause hospitalisations, ICU admissions, and deaths in Hong Kong between 2004 and 2012 were obtained from the Department of

Health and the Census and Statistics Department of the Government of the Hong Kong SAR. The public health laboratory in Hong Kong receives specimens for diagnostic and surveillance purposes from sentinel outpatient clinics and local hospitals, and reports the weekly proportions of specimens that tested positive for common respiratory viruses, including influenza (by type and subtype), respiratory syncytial virus, parainfluenza and adenovirus. The Centre for Health Protection reported weekly proportions of general practitioner consultations due to ILI. Weekly mean temperature and relative humidity were extracted from the published data from the Hong Kong Observatory. Age-specific population size from 2004 to 2012 was obtained from the Census and Statistics Department.

Statistical analyses

Using results from virological testing on the nasal and throat specimens collected from randomly selected household members in Hong Kong in the cohort study in 2009 to 2012, we were able to derive the proportion of infections with each virus among individuals in different age groups during the time period when the subjects were recruited and followed up. The number of individuals infected with each virus in Hong Kong during the same period as when the cohort study did was derived from the probability of infection by weighting the differences in age distribution between the cohort and general Hong Kong population.

We fitted weekly all-cause hospitalisation, ICU admissions, and death rates separately to multiple linear regression models that allow for adjustment of activities of different respiratory viruses, meteorological parameters, and temporal trends in weekly rates during the study period. The excess hospitalisations, ICU admissions and deaths associated with a respiratory virus were estimated as the difference between the predicted rates in the presence and in the absence of activities of the virus. These models were each run for age groups 1 (age 0-5 years) and 2 (age 6-15 years) using only respiratory causes of death (ICD-10 codes J00-99).

We estimated the number of cases for each severity level to derive the probability of medically attended symptomatic infection, the probability of hospitalisation among all medically attended symptomatic infections, the probability of being admitted to ICU after hospitalisation, and the probability of death after being admitted to ICU and to construct the impact pyramid for each common respiratory virus of interest applied a Bayesian evidence synthesis approach to integrate relevant information to derive the above parameters for each virus.^{8,9} Information on the observed number of events in each level of the impact pyramid was used to derive the posterior distribution for each

parameter. We used flat non-informative priors for each parameter. The model was fitted with Markov chain Monte Carlo to make inference on the parameters, with 100 000 iterations after burn-in. The advantage of this approach is that it maintains uncertainty from each data source through to the final estimates of the severity profile of each virus.

Results

During 2009 to 2012, influenza viruses caused three winter waves secondary to seasonal influenza A(H1N1) virus in 2009, the newly emerged influenza A(H1N1)pdm09 virus in 2011, and influenza B in 2012, and three summer waves associated with influenza A(H1N1)pdm09 virus in 2009 and influenza A(H3N2) in 2010 and 2012. No apparent seasonal patterns were suggested by virus activity data collected from the local sentinel surveillance system. Instead viruses were detected throughout the whole year except that a 3- to 4-year cyclic pattern was observed for adenovirus.

Respiratory symptomatic infections were estimated based on data collected from the prospective cohort. Viruses were more frequently detected in older children compared to the young counterparts. Among children who were testing positive for any of the six viruses, the distribution of acute respiratory symptoms varied substantially (data not shown). In the prospective cohort, we estimated that approximately 75% to 8% of healthy children aged 0 to 15 years would present acute respiratory symptoms associated with infection with influenza virus, syncytial virus, parainfluenza and adenovirus each year.

A telephone survey was conducted in order to collect information on health-seeking behaviour among children who presented acute respiratory symptoms in Hong Kong. In total, 1002 parents/guardians who were caring for at least one child aged 0 to 15 years were recruited for interview. Respondents recruited in the survey reported that >20% of their children showed at least one of the acute respiratory symptoms in the past months before the interview. Cough, running nose, and sore throat were the most frequent. We derived the probability for medical consultation for each symptom combination based on symptoms reported by each subject (data not shown).

We used linear regression models to fit weekly respiratory hospitalisation, ICU admission and death rates in 2009 to 2012, and estimated the excess respiratory hospitalisation, ICU and death associated with each of the six types/subtypes of respiratory viruses in children aged 0 to 5 years and 6 to 15 years between 2009 and 2012. The average annual excess hospitalisation admission rate was particularly high in respiratory infections associated with influenza and respiratory syncytial virus, 646

TABLE 1. Estimated annual rates (per 100 000) of symptomatic and medically attended symptomatic respiratory infections, excess hospitalisations, intensive-care-unit (ICU) admissions and deaths due to respiratory infections attributable to 7 types/subtypes of common respiratory viruses in children aged 0 to 5 years and 6 to 15 years between 2009 and 2012.

	Estimated annual rates (per 100 000) [95 % confidence interval]				
	Symptomatic*	Medically attended*	Excess hospitalisation	Excess ICU admission	Excess death
Age 0-5 years					
All respiratory viruses	6847 (0-22709)	5432 (0-18368)	1491 (1359-1621)	27 (16-38)	-2.83 (-5.33 to -0.54)
All flu	2074 (0-8540)	1875 (0-7737)	646 (587-704)	0.8 (-2.6 to 4.1)	0.25 (-0.45 to 1.01)
A/h3	323 (0-1883)	300 (0-1748)	299 (270-328)	1.8 (0.3-3.3)	-0.06 (-0.40 to 0.27)
A/ph1	782 (0-2902)	703 (0-2609)	163 (155-172)	-0.3 (-0.7 to 0.2)	-0.21 (0.26 to -0.15)
B	970 (0-3756)	873 (0-3381)	119 (93-144)	-2.6 (-4.3 to -1.0)	0.05 (-0.31 to 0.41)
Respiratory syncytial virus	2538 (0-6961)	1716 (0-4706)	686 (623-747)	20 (17-23)	-0.47 (-1.22 to 0.26)
Parainfluenza	1705 (0-4915)	1415 (0-4078)	124 (63-185)	6.3 (0.4-12)	-0.85 (-2.20 to 0.42)
Adenovirus	528 (0-2293)	426 (0-1847)	35 (0-69)	-0.2 (-6.2 to 6.2)	-1.76 (-3.25 to -0.44)
Age 6-15 years					
All respiratory viruses	7570 (0-16205)	6230 (0-13256)	312 (264-359)	4.5 (1.3-7.7)	0.30 (0.00-1.15)
All flu	5208 (592-10602)	4426 (469-8909)	220 (205-235)	1.2 (0.2-2.1)	0.08 (0.00-0.83)
A/h3	931 (0-2086)	847 (0-1872)	48 (41-55)	-0.2 (-0.7 to 0.2)	-
A/ph1	1381 (0-2780)	1154 (0-2324)	107 (104-109)	1.2 (1.1-1.3)	0.11 (0.00-0.95)
B	2896 (832-5737)	2425 (684-4713)	89 (82-97)	0.6 (0.1-1.1)	0.05 (0.00-0.41)
Respiratory syncytial virus	853 (0-2069)	608 (0-1474)	8 (-7-23)	-0.1 (-1.0 to 0.8)	-
Parainfluenza	1079 (0-2367)	849 (0-1932)	37 (11-63)	1.2 (-0.6 to 3.1)	0.31 (0.00-1.16)
Adenovirus	430 (0-1167)	346 (0-940)	47 (22-72)	2.2 (0.2-4.1)	-

* Negative estimates of the lower bound of the 95% CIs were truncated to zero

and 686 per 100 000 population in children aged 0 to 5 years whereas parainfluenza caused a lower excess hospitalisation burden comparable to influenza A(H1N1)pdm09 or B viruses, and adenovirus was associated with the lowest excess hospitalisations in this age group (Table 1). In older children, most excess hospitalisations and ICU admissions associated with respiratory infections were likely to be caused by influenza, followed by adenovirus and parainfluenza. Among influenza viruses, influenza A(H1N1)pdm09 contributed a larger proportion of the excess hospitalisation burden than other types/subtypes. In general, no substantial excess deaths were estimated the excess ICU admissions were estimated to be considerably higher in younger than older children across different virus types/subtypes.

We estimated the severity of respiratory infections with seven types/subtypes of commonly reported respiratory viruses in Hong Kong from 2009 through 2012 using a Bayesian synthetic framework to incorporate information derived from different data sources. To estimate the proportion of symptomatic infections seeking health care, progressing to being hospitalised, ICU admission or death, the number of patients in each level of the severity pyramid was estimated (Fig). We estimated

the proportion of respiratory deaths, ICU admissions, and hospitalisations among symptomatic and medically-attended symptomatic infections with influenza A(H1N1)pdm09, A(H3N2), B, respiratory syncytial virus, parainfluenza, and adenovirus (Table 2).

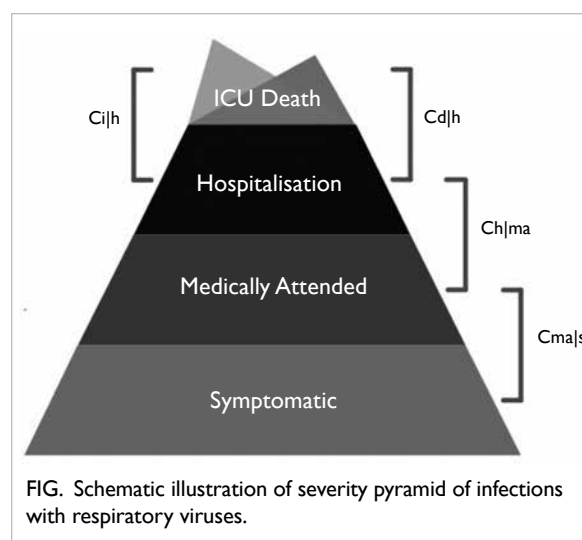


FIG. Schematic illustration of severity pyramid of infections with respiratory viruses.

TABLE 2. Estimated ratios of respiratory death, intensive care unit (ICU) admission and hospital admission among symptomatic or medically attended symptomatic infections with six common respiratory virus types/subtypes in children aged 0 to 5 years and 6 to 15 years.

	Estimated ratio (95 % confidence interval)						
	Symptomatic: medically-attended	Hospitalised: medically-attended	ICU admitted: hospitalised	Fatal: hospitalised	Hospitalised: symptomatic	ICU admitted: symptomatic	Fatal: symptomatic
Age 0-5 years							
All viruses	0.79 (0.762-0.793)	0.27 (0.259-0.288)	0.02 (0.014-0.028)	-	0.22 (0.207-0.230)	0.004 (0.003-0.007)	-
All flu	0.90 (0.849-0.910)	0.34 (0.313-0.375)	0.001 (0.000-0.005)*	0.0004 (0.0000-0.0015)	0.31 (0.283-0.337)	0.0004 (0.000-0.002)*	0.0001 (0.0000-0.0015)
A/h3	0.91 (0.833-0.992)	0.99 (0.825-1.000)	0.006 (0.000-0.011)*	-	0.93 (0.773-1.058)	0.006 (0.003-0.028)	-
A/ph1	0.90 (0.821-0.922)	0.23 (0.195-0.275)	-	-	0.21 (0.174-0.245)	-	-
B	0.90 (0.864-0.957)	0.14 (0.108-0.160)	-	0.0004 (0.0000-0.0278)	0.12 (0.095-0.141)	-	0.0004 (0.0000-0.0031)
Respiratory syncytial virus	0.75 (0.721-0.771)	0.40 (0.364-0.433)	0.03 (0.018-0.044)	-	0.27 (0.243-0.287)	0.008 (0.007-0.015)	-
Parainfluenza	0.83 (0.817-0.883)	0.09 (0.068-0.100)	0.05 (0.017-0.102)	-	0.07 (0.056-0.082)	0.004 (0.002-0.009)	-
Adenovirus	-	0.08 (0.046-0.096)	-	-	0.07 (0.037-0.078)	-	-
Age 6-15 years							
All viruses	0.82 (0.810-0.839)	0.05 (0.042-0.054)	0.01 (0.003-0.026)	0.001 (0.0000-0.0103)	0.04 (0.035-0.044)	0.0006 (0.0001-0.001)	0.00004 (0.00000-0.00040)
All flu	0.85 (0.829-0.869)	0.05 (0.042-0.056)	0.006 (0.000-0.024)*	0.0004 (0.0000-0.0154)	0.04 (0.036-0.047)	0.0002 (0.000-0.001)*	0.00002 (0.00000-0.00059)
A/h3	0.91 (0.853-0.944)	0.06 (0.042-0.077)	-	-	0.05 (0.039-0.070)	-	-
A/ph1	0.84 (0.798-0.871)	0.09 (0.073-0.111)	0.01 (0.000-0.045)*	0.001 (0.0000-0.0357)	0.08 (0.062-0.093)	0.0009 (0.000-0.005)*	0.00008 (0.00000-0.00217)
B	0.84 (0.802-0.851)	0.04 (0.029-0.046)	0.007 (0.000-0.041)*	0.0006 (0.0000-0.0500)	0.03 (0.024-0.037)	0.0002 (0.000-0.001)*	0.00002 (0.000000-0.00104)
Respiratory syncytial virus	0.71 (0.618-0.761)	0.01 (0.002-0.016)	-	-	0.01 (0.001-0.011)	-	-
Parainfluenza	0.79 (0.762-0.839)	0.04 (0.033-0.065)	0.03 (0.000-0.178)*	0.008 (0.0000-0.1334)	0.03 (0.027-0.051)	0.001 (0.000-0.005)*	0.0003 (0.00000-0.00465)
Adenovirus	0.81 (0.69-0.911)	0.14 (0.098-0.183)	0.05 (0.000-0.132)*	-	0.11 (0.079-0.145)	0.005 (0.000-0.015)*	-

* The negative lower bound of the 95% confidence intervals was truncated to zero. The numerator and/or denominator used to calculate the proportion were/was negative

Discussion

There was a substantial burden of symptomatic respiratory infections associated with influenza, respiratory syncytial virus, parainfluenza, and adenovirus each year in children aged 0 to 15 years in Hong Kong. Among those presenting with acute respiratory symptoms, approximately 70% to 90% of patients choose to seek a medical consultation either through government-supported public clinics/hospitals or general practitioners/private hospitals. No major differences were observed between young and older children. During 2009 to 2012, the annual excess hospitalisation rate was different for each respiratory virus of interest, whereas the excess

burden of ICU admission and death associated with respiratory infections of the virus was generally low or rare in both younger and older children, consistent with previous findings.¹⁰ Therefore, severity of respiratory infection measured by the risk of ICU admission and death was extremely low among sick children having symptomatic infections with the six types/subtypes of respiratory viruses in Hong Kong.

Our study indicated that it was possible to quantitatively measure the severity of infections with respiratory viruses using data collected from the sentinel surveillance system, community-based cohort and population morbidity and mortality statistics. Previously published studies to measure

population burden of infections associated with respiratory infection largely relied on outpatient data collected from outpatient clinics or one cohort of subjects (patients or non-patients) in which it was therefore difficult to determine the population denominator for estimation of the severity profile, or used rate difference statistical models which would sometimes fail to estimate virus-specific burden when there was co-circulation of viruses during the study period.¹⁰

Conclusion

Considerable respiratory morbidity burden was caused by common respiratory viruses in Hong Kong children, and severity of infection varied across different viruses in young and old children. Influenza viruses generally contributed to the highest disease burden in both young and old children. Respiratory syncytial virus was associated with the highest risk of hospitalisation among laboratory-confirmed symptomatic infections in children aged 0 to 5 years.

Funding

This study was supported by the Health and Medical Research Fund, Food and Health Bureau, Hong Kong SAR Government (#13120802). The full report is available from the Health and Medical Research Fund website (<https://rfs1.fhb.gov.hk/index.html>).

Disclosure

The results of this research have been previously published in:

(1) Wu P, Presanis AM, Bond HS, Lau EHY, Fang VJ, Cowling BJ. A joint analysis of influenza-associated hospitalizations and mortality in Hong Kong, 1998–2013. *Sci Rep* 2017;7:929.

References

1. Gaunt ER, Harvala H, McIntyre C, Templeton KE, Simmonds P. Disease burden of the most commonly detected respiratory viruses in hospitalized patients calculated using the disability adjusted life year (DALY) model. *J Clin Virol* 2011;52:215-21.
2. Khor CS, Sam IC, Hooi PS, Quek KE, Chan YF. Epidemiology and seasonality of respiratory viral infections in hospitalized children in Kuala Lumpur, Malaysia: a retrospective study of 27 years. *BMC Pediatr* 2012;12:32.
3. Pogka V, Kossivakis A, Kalliaropoulos A, et al. Respiratory viruses involved in influenza-like illness in a Greek pediatric population during the winter period of the years 2005-2008. *J Med Virol* 2011;83:1841-8.
4. Chiu SS, Chan KH, Chen H, et al. Virologically confirmed population-based burden of hospitalization caused by respiratory syncytial virus, adenovirus, and parainfluenza viruses in children in Hong Kong. *Pediatr Infect Dis J* 2010;29:1088-92.
5. Cowling BJ, Fang VJ, Nishiura H, et al. Increased risk of noninfluenza respiratory virus infections associated with receipt of inactivated influenza vaccine. *Clin Infect Dis* 2012;54:1778-83.
6. Cowling BJ, Ng S, Ma ES, et al. Protective efficacy of seasonal influenza vaccination against seasonal and pandemic influenza virus infection during 2009 in Hong Kong. *Clin Infect Dis* 2010;51:1370-9.
7. Gadsby NJ, Hardie A, Claas EC, Templeton KE. Comparison of the Luminex Respiratory Virus Panel fast assay with in-house real-time PCR for respiratory viral infection diagnosis. *J Clin Microbiol* 2010;48:2213-6.
8. Presanis AM, Pebody RG, Paterson BJ, et al. Changes in severity of 2009 pandemic A/H1N1 influenza in England: a Bayesian evidence synthesis. *BMJ* 2011;343:d5408.
9. Presanis AM, De Angelis D, New York City Swine Flu Investigation Team, et al. The severity of pandemic H1N1 influenza in the United States, from April to July 2009: a Bayesian analysis. *PLoS Med* 2009;6:e1000207.
10. Monto AS. Occurrence of respiratory virus: time, place and person. *Pediatr Infect Dis J* 2004;23(1 Suppl):S58-64.

C-terminal truncated hepatitis B virus X protein regulates tumorigenicity, self-renewal, and chemoresistance via STAT3/Nanog signalling pathway: abridged secondary publication

RHH Ching, KMF Sze, EYT Lau, YT Chiu, JMF Lee, IOL Ng, TKW Lee *

KEY MESSAGES

1. HBx- Δ C1 (a major C-terminal truncated form reported with a breakpoint at 130aa) regulates cancer stem cell properties including tumour initiation, self-renewal, drug resistance, and invasiveness.
2. HBx- Δ C1 regulates liver cancer stem cells through Stat3/Nanog cascade, which provides a new insight for the therapeutic intervention for hepatitis B virus-related hepatocellular

carcinoma.

Hong Kong Med J 2020;26(Suppl 4):S22-5
HMRF project number: 13120892

RHH Ching, KMF Sze, EYT Lau, YT Chiu, JMF Lee, IOL Ng, TKW Lee

Li Ka Shing Faculty of Medicine, The University of Hong Kong, Hong Kong; State Key Laboratory for Liver Research & Department of Pathology

* Principal applicant and corresponding author: terence.kw.lee@polyu.edu.hk

Introduction

Hepatocellular carcinoma (HCC) is the fifth most common cancer worldwide. Hepatitis B virus (HBV) DNA is often integrated and highly rearranged within the host DNA in HCC. These templates frequently produce the HBV viral oncoprotein (HBx), which is active in transactivation assays. The sustained production of HBx is associated with hepatocellular transformation and represents a major contribution of HBV to HCC.¹ HBV integration is detected in 80% to 90% of host genomes from HBV-infected HCC cases, and the HBx gene is partially deleted frequently during the integration process, causing the C-terminal truncation of HBx.^{2,3} In addition, C-terminally truncated HBx (HBx- Δ C) plays a critical pro-oncogenic role in hepatocarcinogenesis and metastasis.^{2,3} These results demonstrate that, in addition to the full-length HBx, the HBx- Δ C also plays an important role in HCC development. Among various truncated mutants of HBx, c-terminal truncation with a breakpoint of 130aa (HBx- Δ C1) is the major truncated form of HBx existing in our HCC samples.³ However, the molecular mechanism whereby HBx- Δ C1 contributes to HCC remains largely unknown. Recent evidence supports the existence of cancer stem cell (CSC) / tumour-initiating cell (T-IC) model in leukaemia and a wide range of solid tumours, including HCC.⁴ CSCs are believed to possess both cancer cell- and stem cell-like characteristics, including tumour initiation, self-renewal, and differentiation. HBV can induce stem cell-like and CSC-like signatures in HCC. Despite these findings, direct evidence demonstrating a functional role for HBx- Δ C in promoting liver

carcinogenesis and through regulation of stemness factors in HCC is lacking, and the molecular mechanisms are unknown. In this study, we aim to evaluate the clinical relevance and prognostic significance of stemness factors and HBx- Δ C1 expression at different HCC development stages in the presence or absence of HBV infection and delineate the role of HBx- Δ C1 in regulating Nanog and its tumour-initiating properties.

Methods

Total RNA of human HCC liver tissues was extracted using TRIzol (Invitrogen, Carlsbad, CA), according to manufacturer's protocol. For polymerase chain reaction (PCR) amplification of HBx, sets of PCR primers (1425F: 5'-TCCTTTGTTTACGTCCCGTC-3'; 1840R: 5'-TTAGGCAGAGGTGAAAAAGTTG-3' and 1661R: 5'-GAATTCCTTATGTAAGACCTTGGGCAACAT-3') were used for full-length and COOH-truncated HBx, respectively.

Full-length HBx DNA (GenBank no.: U95551) was amplified from the HBx/pcDNA3.1+ plasmid³ and sub-cloned into Myc/pLVX-Tight Puro and Myc/pcDNA3.1+ vectors. HBx truncation mutant (named HBx- Δ C1) with 24 C-terminal amino acid of HBx deleted was made and sub-cloned into Myc/pLVX-Tight Puro and Myc/pcDNA3.1+ vectors. Bel-7402 and SMMC-7721 cell line were first transfected with pLVX Tet-On Advanced vector (Clontech Laboratories, Mountain View [CA], USA) using Lipofectamine 2000 (Invitrogen), according to manufacturer's protocol. tTA(Tet-On)-expressing Bel-7402 and SMMC-7721 cells were selected

with G418 at 700 µg/mL and 400 µg/mL for 14 days, respectively. To obtain stable inducible HBx-expressing cells, lentivirus containing full-length and C-terminal truncated HBx in Myc/pLVX-Tight Puro vector was infected into tTA-expressing Bel-7402 and SMMC-7721 cells and selected with puromycin at 1 µg/mL for 7 days. In vitro and in vivo functional assays were used to evaluate the effect of transgene on self-renewal, tumorigenicity, drug resistance, and cell migration.

The effect of HBx and HBx-ΔC1 on Stat3/Nanog signalling pathway in both Bel-7402 and SMMC-7721 was evaluated by western blot analysis using specific antibodies against Stat3, p-Stat3 (Y705), and Nanog. The specific effect on Stat3 activation was further evaluated by immunofluorescence staining. The involvement of Stat3 in HBx-ΔC1-mediated self-renewal was investigated by a rescue experiment using Stat3 inhibitor (S3I-201). The clinical correlation between HBx-ΔC1 and Nanog was investigated in a cohort of 107 HCC patient samples by semi-quantitative RT-PCR analysis of HBx and HBx-ΔC1 as described above and qPCR analysis using specific primer of Nanog (F: 5'- CCTGTG ATTTGTGGGCCTG-3', R: 5'- GACAGTCTC CGTGTGAGGCAT-3'). Student's t was used for continuous data wherever appropriate. A P value of <0.05 was considered statistically significant.

Results

HBx- ΔC1 is correlated with stemness factors including Sox2/Nanog

Using lentiviral based Tet-On overexpression approach, we established inducible expression of HBx-FL and HBx-ΔC1 in Bel-7402 and SMMC-7721 cells upon addition of doxycycline at 1 µg/mL. By qPCR analysis, we found preferential induction of certain stemness related genes, including Nanog, Sox2, SMO, and ABCB5, in HBx-ΔC1 expressing HCC cells, when compared with HBx-FL and empty vector control. Interestingly, we found that overexpression of HBx-ΔC1 increased the expression of liver CSC markers including CD133 and CD47 when compared with control and HBx-FL expression in Bel-7402 and SMMC-7721 by qPCR and flow cytometry analyses. In a cohort of 107 HCC patient samples, we examined the expression of Klf4, c-myc, Oct4, β-catenin, Nanog, and Sox2 in HCC clinical samples by qPCR. Consistently, Nanog and Sox2 expression was up-regulated in tumour samples detected with HBx-ΔC1 when compared to those with full length of HBx and without HBV infection.

HBx- ΔC1 overexpression induced CSC properties in HCC

Upon transfection of HBx and HBx-ΔC1 into

Bel7402 and SMMC-7721, HBx-ΔC1 transfectants exhibited increased self-renewal ability, as evidenced by the increase in the number and size of the spheres formed in sphere formation assay. We then examined whether C-terminal truncated form of HBx was more tumorigenic than full length of HBx in vivo by tumour forming assay with HBx-FL expressing and HBx-ΔC1 expressing Bel-7402 and SMMC-7721 cells. Cells at density of 5000, 10000 and 50000 were inoculated subcutaneously into NOD/SCID mice. A significant increase in tumour incidence and size was observed in HBx-ΔC1 expressing cells when compared with control and HBx-FL expressing cells. Our previous studies demonstrated that liver CSCs were more chemoresistant to chemotherapeutic drugs.⁴ Thus, we assessed whether HBx-ΔC1 conferred chemoresistance to HCC cells. We treated transfectants of control, HBx-FL, and HBx-ΔC1 derived from Bel-7402 and SMMC-7721 with cisplatin and doxorubicin and subjected them to Annexin V staining assay. HBx-ΔC1 transfectants were more chemoresistant to cisplatin and doxorubicin when compared with EV and HBx-FL transfectants in both Bel-7402 and SMMC-7721 cells. In addition, overexpression of HBx-ΔC1 conferred greater migratory ability when compared with control and HBx-FL overexpression. Previously, we found that liver CSCs were enriched upon sorafenib treatment, as evidenced by increase in abilities in self-renewal and tumorigenicity in sorafenib-resistant cells.⁵ Based on this finding, we hypothesise that HBx-ΔC1 overexpressing cells are more resistant to sorafenib treatment. We compared the sensitivity of sorafenib among transfectants of control, HBx-FL, and HBx-ΔC1 derived from Bel-7402 and SMMC-7721. By Annexin V staining, HBx-ΔC1 transfectants were more resistant to sorafenib when compared with EV and HBx-FL transfectants in both Bel-7402 and SMMC-7721 cells

HBx-ΔC1-driven tumour initiation and self-renewal through Stat3-Nanog signalling.

Previously, we found that Stat3-Nanog pathway was activated in liver CSCs contributing to tumorigenicity and stemness.⁴ In addition, Stat3 signalling activity was enhanced in HBx expressing cells and HBx transgenic mice leading to carcinogenesis, and therefore, we explored whether Stat3-mediated Nanog regulation was involved in truncated HBx-induced stemness. By western blotting, HBx-ΔC1 preferentially induced expression of Stat3 (Y705) and stem cell transcriptional factor, Nanog, in Bel-7402 and SMMC-7721. We determined Stat3 activity by qualifying p-Stat3 (Y705) level using immunofluorescence staining. Consistently, HBx-ΔC1 stimulated stat-3 activity indicated by higher fluorescent intensity for p-Stat3

(Y705) staining when compared with control and HBx-FL. To further examine whether the HBx-induced response is stat3 dependent, we examined p-Stat3 (Y705) and Nanog expression in response to a STAT3 inhibitor (S3I-201) in Bel-7402 and SMMC-7721 cells. By XTT assay, the cytotoxic effect of Stat3 inhibitor on Bel-7402 and SMMC-7721 cells was examined and IC₅₀ was around 575 μ M and 700 μ M, respectively. By western blot analysis, Nanog expression was downregulated upon S3I-201 treatment. Addition of S3I-201 led to abolishment of HBx-induced self-renewal indicated by the sphere-forming assay. Taken together, these findings suggest that HBx- Δ C1 regulates liver CSCs through Stat3-mediated Nanog regulation.

Discussion

Recent evidence supports the presence of CSCs contributing to resistance to conventional therapies and tumour relapse. HBx has been implicated as playing an oncogenic role in the development of HBV-associated HCC. Recent studies have reported that HBx-enhanced expression of stemness and CSC markers including Oct4, Nanog, Klf-4, and EpCAM in vitro and in vivo contributes to HCC. Consistent to previous findings, we found that HBx enhanced expression of stemness genes including Nanog, Sox2, SMO, and ABCB5. COOH-truncated form of HBx has been shown to have more aggressive behaviour in the development of HCC. In this study, in addition to full length of HBx, we also study the role of COOH-truncated HBx, with a breakpoint at 130aa (HBx- Δ C1) in regulation of cancer stemness. Interestingly, we demonstrated that HBx- Δ C1 regulated the liver CSC properties including enhanced expression of stemness genes, self-renewal capacity, and resistance to chemotherapeutic drugs, and driving tumorigenesis; the effect is more prominent than HCC cells transfected with full length of HBx. These results have demonstrated the distinct role of HBx- Δ C1 in regulation of liver CSCs. In addition, we showed that X gene of HBV integrated into the host liver DNA prior to the appearance of tumour, perhaps up-regulation of stemness factors such as Sox2 and Nanog would be more important to tumour pathogenesis at an early, preneoplastic stage. However, the use of the stemness factors for diagnostic and prognostic purpose is limited by low abundance in HCC samples. Cross-talks of stemness factors have been reported to regulate the stemness of HCC. For instance, Oct4 was found to regulate β -catenin activation in non-canonical manner.⁶ In addition, Oct4 was found to regulate chemoresistance through regulation of Akt pathway.⁷

By western blot analysis and immunofluorescence staining, we found upregulation of nuclear stat3, p-Stat3 and Nanog expression in

HBx-expression cells. We found that Stat3-Nanog signalling pathway was preferentially activated in HBx- Δ C1 transfectants, which was indicated by the enhanced activity of Stat3 and expression of Nanog observed in HBx- Δ C1-expressing Bel-7402 and SMMC-7721 cells, when compared with HBx-FL and control cells. Furthermore, the role of HBx- Δ C1-induced self-renew was further confirmed by treatment of Stat3 inhibitor. We found that the inhibition of Stat3 activation using a Stat3 specific inhibitor abrogated the effect of the HBx- Δ C1-induced self-renewal capacity. These findings suggest that Stat3-Nanog signalling plays a crucial role in regulating the stemness properties mediated by HBx- Δ C1.

Conclusion

HBx- Δ C1 plays critical role in HCC development and progression via the regulation of cancer stemness, which involves preferential activation of the Stat3-Nanog pathway. A better understanding of the molecular mechanism of HBx- Δ C1 will improve our knowledge of HCC pathogenesis, with the goal of developing more-effective management. Our data give a new insight on developing targeted therapies against HBx- Δ C1-induced Nanog and identifying novel markers to predict disease outcome and tumour recurrence.

Funding

This study was supported by the Health and Medical Research Fund, Food and Health Bureau, Hong Kong SAR Government (#13120892). The full report is available from the Health and Medical Research Fund website (<https://rfs1.fhb.gov.hk/index.html>).

Disclosure

The results of this research have been previously published in:

(1) Ching RHH, Sze KMF, Lau EYT, et al. C-terminal truncated hepatitis B virus X protein regulates tumorigenicity, self-renewal and drug resistance via STAT3/Nanog signaling pathway. *Oncotarget* 2017;8:23507-16.

References

1. Lee TK, Man K, Poon RT, et al. Signal transducers and activators of transcription 5b activation enhances hepatocellular carcinoma aggressiveness through induction of epithelial-mesenchymal transition. *Cancer Res* 2006;66:9948-56.
2. Ma NF, Lau SH, Hu L, et al. COOH-terminal truncated HBV X protein plays key role in hepatocarcinogenesis. *Clin Cancer Res* 2008;14:5061-8.
3. Sze KM, Chu GK, Lee JM, Ng IO. C-terminal truncated hepatitis B virus x protein is associated with metastasis and enhances invasiveness by C-Jun/matrix metalloproteinase

- protein 10 activation in hepatocellular carcinoma. *Hepatology* 2013;57:131-9.
4. Lee TK, Castilho A, Cheung VC, Tang KH, Ma S, Ng IO. CD24(+) liver tumor-initiating cells drive self-renewal and tumor initiation through STAT3-mediated NANOG regulation. *Cell Stem Cell* 2011;9:50-63.
 5. Lo J, Lau EY, Ching RH, et al. Nuclear factor kappa B-mediated CD47 up-regulation promotes sorafenib resistance and its blockade synergizes the effect of sorafenib in hepatocellular carcinoma in mice. *Hepatology* 2015;62:534-45.
 6. Chai S, Ng KY, Tong M, et al. Octamer 4/microRNA-1246 signaling axis drives Wnt/ β -catenin activation in liver cancer stem cells. *Hepatology* 2016;64:2062-76.
 7. Wang XQ, Ongkeko WM, Chen L, et al. Octamer 4 (Oct4) mediates chemotherapeutic drug resistance in liver cancer cells through a potential Oct4-AKT-ATP-binding cassette G2 pathway. *Hepatology* 2010;52:588-39.

Involvement of autophagy in antibacterial actions of vitamin D in *Helicobacter pylori* infection: abridged secondary publication

W Hu, L Zhang, WKK Wu, CH Cho

KEY MESSAGES

1. We identified a unique pathogenic mechanism on how *Helicobacter pylori* can survive by hiding inside the autophagosomes in cells.
2. We discovered a novel antibacterial signalling pathway of VD3 through the activation of PDIA3/STAT3 - MCOLN3 - Ca²⁺ axis, to reactivate the lysosomal acidification and degradation function of autolysosomes, which is the key signal pathway for the antibacterial action of VD3 both in cells and in animals and perhaps further in humans.

Hong Kong Med J 2020;26(Suppl 4):S26-8
HMRF project number: 13120062

¹ W Hu, ^{1,2} L Zhang, ^{1,2} WKK Wu, ^{3,4} CH Cho

¹ Department of Anaesthesia and Intensive Care, The Chinese University of Hong Kong, Hong Kong

² Institute of Digestive Diseases, State Key Laboratory of Digestive Diseases, LKS Institute of Health Sciences, CUHK Shenzhen Research Institute, The Chinese University of Hong Kong, Hong Kong

³ School of Biomedical Science, The Chinese University of Hong Kong, Hong Kong

⁴ Laboratory of Molecular Pharmacology, Department of Pharmacology, School of Pharmacy, Southwest Medical University, Luzhou, Sichuan, China

* Principal applicant and corresponding author: chcho@cuhk.edu.hk

Helicobacter pylori is a Gram-negative spiral bacterium that has colonised over 50% of the world's population as a result of constant failure in *H pylori* clearance by the host immune system in the upper gastrointestinal tract.¹ Worse, the globally accepted triple therapy (comprising a proton pump inhibitor plus two antibiotics) is challenged by a steady increase in *H pylori* resistance to classical antibiotics, especially to clarithromycin.² It has been suggested that the inefficacy in pathogen eradication is due to the capacity of *H pylori* for hiding inside host cells,^{3,4} thereby escaping from the innate response by immune cells. Although the precise mechanisms of immune evasion remain obscure, increasing evidence suggests that autophagy plays an important role in the pathogenesis of *H pylori*-associated gastric disorders.^{5,6}

Autophagy, characterised by the formation of double-membrane vesicles designated as autophagosomes, is an evolutionarily conserved self-degradation process utilised by host cells to maintain cellular homeostasis and protect against invading pathogens.⁷ Lysosomes are membrane-bound organelles that contain over 50 different degradative hydrolases. By fusing with lysosomes, autophagosomes mature into autolysosomes, in which they sequester pathogens followed by degradation by lysosomal proteases.⁸ Initially, the autophagic pathway was regarded as the host defence strategy against invading pathogens, as several microbes such as *Listeria monocytogenes* were captured by autophagosomes, and then degraded

to avoid persistent infection.⁹ However, emerging evidence underlines an unexpected behaviour of bacteria to disrupt such a defensive autophagic process, allowing active intracellular replication.¹⁰ *H pylori* has been proved to induce autophagy in several gastric cell lines.¹¹ A suppressive function of *H pylori*-vacuolating cytotoxin in the autophagosome maturation was revealed,¹² suggesting that the bacterium might utilise these intracellular compartments to hibernate and further replicate for a long-term survival in the gastric mucosa. However, the molecular mechanisms by which *H pylori* evades the immune system and the effects of antibiotics need to be elucidated, and novel antibiotics are urgently demanded to efficiently eradicate *H pylori* infection through this unique cellular mechanism. In addition, these agents, if any, could provide a better alternative from the current traditional antibiotics for the treatment of drug-resistant *H pylori*.

In this study, we verified an occurrence of intracellular *H pylori* in normal human gastric epithelial HFE145 cells, and more important, inside the cells of human stomachs. Moreover, we observed that the pathogens were sequestered and survived in non-digestive autophagosomes, which is due to an impaired lysosomal acidification caused by *H pylori* infection. We further showed the involvement of *H pylori* virulence factor CagA in the inhibition of Ca²⁺ channel MCOLN3 protein. Thus, our current results might explain the inefficiency in *H pylori* clearance after the treatment with some membrane-impermeable antibiotics. The survival of bacteria in

disarmed autophagosomes might be a significant reason for *H. pylori* to persist and recur in host stomachs.

Vitamin D3 (VD3) as a steroid hormone is known as a supplement to improve overall human health. Emerging evidence points out a potential antimicrobial activity of VD3 in humans. Indeed, its antimicrobial action against *Mycobacterium tuberculosis* infection has been verified,¹³ even though the precise mechanisms governing this antibacterial activity remain controversial. In the current study, we reported an unexpected antimicrobial effect of VD3 against *H. pylori* colonisation *in vitro* and in mouse stomachs. In contrast to conventional antimicrobial actions induced by VD3 through the production of antimicrobial peptides such as cathelicidin and β -defensin 2,¹⁴ we proved that such antibacterial effect is mediated through PDIA3 receptor but not the classical vitamin D receptor. We further observed that 1,25D3, the active metabolite of VD3, initiated the nuclear translocation of PDIA3/STAT3 complex, and the subsequent transcriptional up-regulation of MCOLN3 channels. All these play a pivotal role in the antimicrobial action of VD3 against *H. pylori*

infection. MCOLN3 channel is predominantly expressed on the late endosomal and lysosomal membranes (>75%).¹⁵ Ca^{2+} release from endolysosome via the MCOLN3 channel is necessary for the lysosomal acidification and maturation.^{15,16} Our results showed a modulatory role of PDIA3/STAT3 complex in the MCOLN3 expression. Moreover, VD3 could up-regulate MCOLN3 channel, which is required for Ca^{2+} release from lysosomes, and then consequently normalised lysosomal acidification. Finally, the repaired digestive machinery operating inside the gastric cells would drive the bacteria to degradation through the revival autolysosomal pathway.

In conclusion, our study identified a unique pathogenic mechanism on how *H. pylori* can survive by hiding inside the autophagosomes in cells. We discovered a novel antibacterial signalling pathway of VD3 through the activation of PDIA3/STAT3 - MCOLN3 - Ca^{2+} axis, to reactivate the lysosomal acidification and degradation function of autolysosomes (Fig), which is the key signal pathway for the antibacterial action of VD3 both in cells and in animals and perhaps further in humans. A

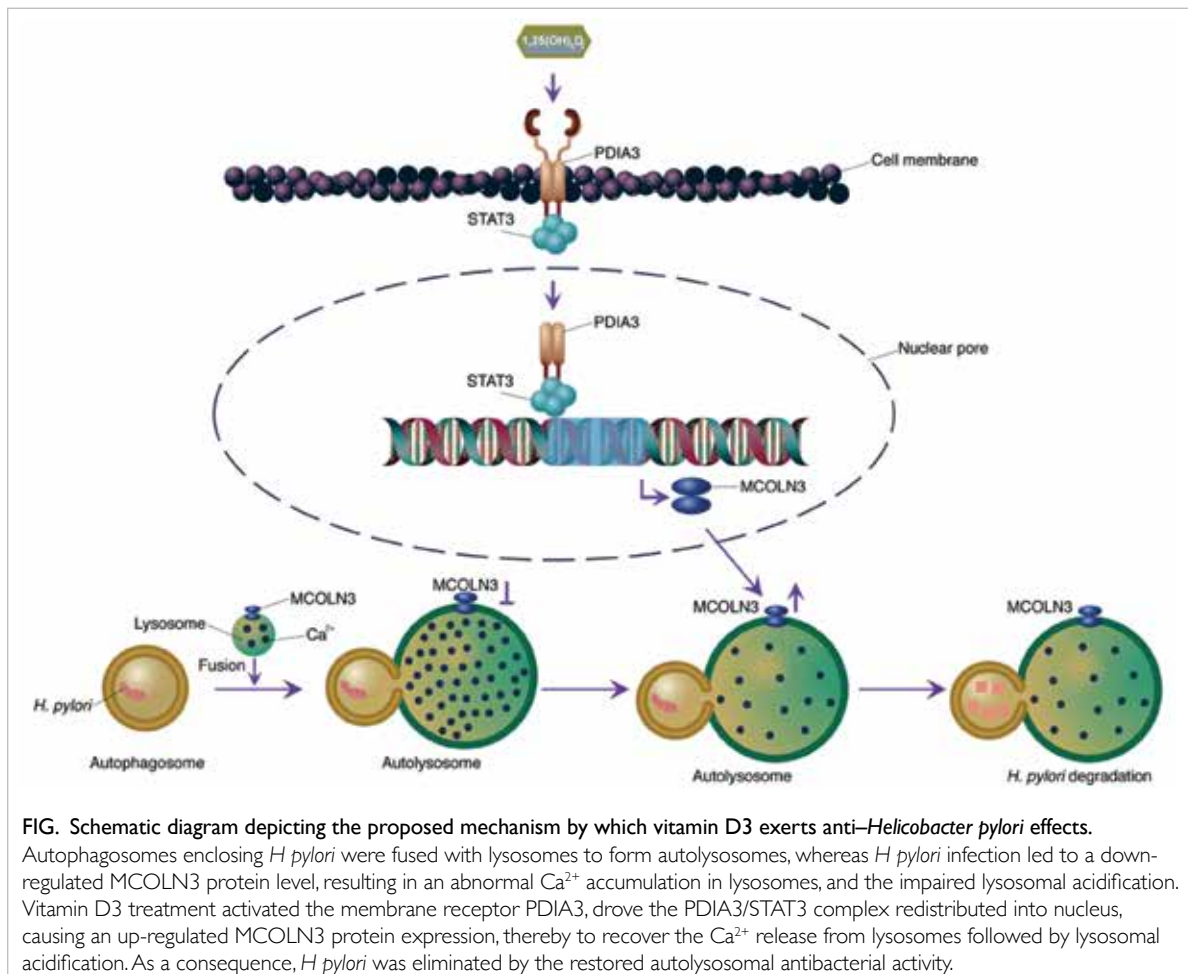


FIG. Schematic diagram depicting the proposed mechanism by which vitamin D3 exerts anti-*Helicobacter pylori* effects.

Autophagosomes enclosing *H. pylori* were fused with lysosomes to form autolysosomes, whereas *H. pylori* infection led to a down-regulated MCOLN3 protein level, resulting in an abnormal Ca^{2+} accumulation in lysosomes, and the impaired lysosomal acidification. Vitamin D3 treatment activated the membrane receptor PDIA3, drove the PDIA3/STAT3 complex redistributed into nucleus, causing an up-regulated MCOLN3 protein expression, thereby to recover the Ca^{2+} release from lysosomes followed by lysosomal acidification. As a consequence, *H. pylori* was eliminated by the restored autolysosomal antibacterial activity.

clinical trial in the Prince of Wales Hospital, Hong Kong is currently underway to demonstrate a new therapeutic application of VD3 in *H pylori* infection and gastritis. Understanding of these mechanisms of action may provide new therapeutic strategies and targets and thereby new therapeutic agents for *H pylori* infection and treatment of its associated diseases in the upper gastrointestinal tract.

Funding

This study was supported by the Health and Medical Research Fund, Food and Health Bureau, Hong Kong SAR Government (#13120062). The full report is available from the Health and Medical Research Fund website (<https://rfs1.fhb.gov.hk/index.html>).

Disclosure

The results of this research have been previously published in:

(1) Hu W, Zhang L, Li MX, et al. Vitamin D3 activates the autolysosomal degradation function against *Helicobacter pylori* through the PDIA3 receptor in gastric epithelial cells. *Autophagy* 2019;15:707-25.

References

1. Fukase K, Kato M, Kikuchi S, et al. Effect of eradication of *Helicobacter pylori* on incidence of metachronous gastric carcinoma after endoscopic resection of early gastric cancer: an open-label, randomised controlled trial. *Lancet* 2008;372:392-7.
2. Thung I, Aramin H, Vavinskaya V, et al. Review article: the global emergence of *Helicobacter pylori* antibiotic resistance. *Aliment Pharmacol Ther* 2016;43:514-33.
3. Allen LA, Schlesinger LS, Kang B. Virulent strains of *Helicobacter pylori* demonstrate delayed phagocytosis and stimulate homotypic phagosome fusion in macrophages. *J Exp Med* 2000;191:115-28.
4. Deen NS, Huang SJ, Gong L, Kwok T, Devenish RJ. The impact of autophagic processes on the intracellular fate of *Helicobacter pylori*: more tricks from an enigmatic pathogen? *Autophagy* 2013; 9:639-52.
5. Chu YT, Wang YH, Wu JJ, Lei HY. Invasion and multiplication of *Helicobacter pylori* in gastric epithelial cells and implications for antibiotic resistance. *Infect Immun* 2010;78:4157-65.
6. Wang YH, Gorvel JP, Chu YT, Wu JJ, Lei HY. *Helicobacter pylori* impairs murine dendritic cell responses to infection. *PLoS One* 2010;5:e10844.
7. Klionsky D, Abdalla FC, Abeliovich H, et al. Guidelines for the use and interpretation of assays for monitoring autophagy. *Autophagy* 2012;8:445-544.
8. He C, Klionsky DJ. Regulation mechanisms and signaling pathways of autophagy. *Annu Rev Genet* 2009;43:67-93.
9. Rich KA, Burkett C, Webster P. Cytoplasmic bacteria can be targets for autophagy. *Cell Microbiol* 2003;5:455-68.
10. Levine B. Eating oneself and uninvited guests: autophagy-related pathways in cellular defense. *Cell* 2005;120:159-62.
11. Terebiznik MR, Raju D, Vázquez CL, et al. Effect of *Helicobacter pylori*'s vacuolating cytotoxin on the autophagy pathway in gastric epithelial cells. *Autophagy* 2009;5:370-9.
12. Raju D, Hussey S, Ang M, et al. Vacuolating cytotoxin and variants in Atg16L1 that disrupt autophagy promote *Helicobacter pylori* infection in humans. *Gastroenterology* 2012;142:1160-71.
13. Campbell GR, Spector SA. Vitamin D inhibits human immunodeficiency virus type 1 and *Mycobacterium tuberculosis* infection in macrophages through the induction of autophagy. *PLoS Pathog* 2012;8:e1002689.
14. Youssef DA, Miller CW, El-Abbassi AM, et al. Antimicrobial implications of vitamin D. *Dermatoendocrinol* 2011;3:220-9.
15. Zeevi DA, Frumkin A, Bach G. TRPML and lysosomal function. *Biochim Biophys Acta* 2007;1772:851-8.
16. Di Palma F, Belyantseva IA, Kim HJ, Vogt TF, Kachar B, Noben-Trauth K. Mutations in *Mcoln3* associated with deafness and pigmentation defects in varitint-waddler (Va) mice. *Proc Natl Acad Sci U S A* 2002;99:14994-9.

Structure-based discovery of inhibitors of *Helicobacter pylori* urease: abridged secondary publication

CL Tam, MH Yuen, YS Nim, YF Xu, SWN Au, JCK Ngo, P Huang, KB Wong *

KEY MESSAGES

1. Structure-based screening was performed by docking >270 000 ligands to the crystal structures of UreG using the program DOCK.
2. Ranked by the calculated binding energies and a clustering analysis, 73 ligands were selected for *in-vitro* enzyme assay.
3. The inhibition against UreG was further improved by screening structural analogues of initial hits. The best inhibitors have IC₅₀ values in the range of 20–30 μM.
4. UreG inhibitors identified, like the urease inhibitor acetohydroxamic acid, could suppress

the survival of *Helicobacter pylori* in acid medium, suggesting that inhibiting the urease maturation could be a novel target for inhibiting the growth of *H pylori* in acid environment.

Hong Kong Med J 2020;26(Suppl 4):S29-31
HMRF project number: 13120122

¹ CL Tam, ¹ MH Yuen, ¹ YS Nim, ² YF Xu, ¹ SWN Au, ¹ JCK Ngo, ² P Huang, ¹ KB Wong

¹ School of Life Sciences, The Chinese University of Hong Kong
² College of Chinese Medicine, Guangzhou University of Chinese Medicine

* Principal applicant and corresponding author: kbwong@cuhk.edu.hk

Introduction

Survival of *Helicobacter pylori* in acid stomach is dependent on the urease activity that produces the neutralising ammonia from the urea.¹ For example, *H pylori* cannot survive in acid medium without the substrate urea or in the presence of urease inhibitors such as acetohydroxamic acid. The biosynthesis of active urease requires a post-translational carbamylation of an active-site lysine residue and insertion of two nickel ions to its active site.² This maturation process is assisted by four urease maturation factors (or urease accessory proteins), namely UreE, UreF, UreG, and UreH. Our research group has determined the crystal structures of the UreG/UreF/UreH complex, which shed insights into the mechanism of urease maturation.² In particular, we demonstrated how the GTP hydrolysis may promote dissociation of the UreG dimer, resulting in the release of nickel.

As the survival of *H pylori* in acid stomach requires the biosynthesis of active urease, we argue that inhibitors of UreG, a GTPase essential to the urease maturation process could be a novel strategy to treat *H pylori* infection. We proposed to use structure-based screening to identify potential inhibitors of UreG, and to screen top-ranked ligand experimentally using an *in-vitro* enzyme assay. We then tested if the UreG inhibitors identified can inhibit the growth of *H pylori* in an acid medium.

Methods

Structure-based screening

The DOCK 6.5 (<http://dock.compbio.ucsf.edu>) was used to perform the docking simulations. Five

independent simulations were performed: four targeting the active site of UreG of the dimeric or the monomeric form of UreG in complex with GDP or GMPPNP, and one targeting the binding surface of UreG/UreF. For each simulation, we docked 273 477 ligands in the SPECS library of the ZINC database. For each simulation, 20 docked ligands were selected for further functional assay by two criteria. First, the docked ligands were ranked according to the binding energies calculated by the DOCK, and the top 10 ranked ligands were selected. Second, the top 1% of the ranked ligands were clustered according to their structural similarity using the ChemMine Tools (<http://chemmine.ucr.edu/>). One representative ligand, with the strongest binding energy, from each of the 10 largest clusters was selected. After checking redundancy and commercial availability, 73 ligands were purchased from SPECS (<http://www.specs.net>) for wet-lab characterisation.

In-vitro enzyme assay

Expression of *H pylori* UreG was performed as described previously.² Zero to 250 μM of selected ligands were added to the enzyme-mix solution (5 μM UreG, 2.5 μM NiSO₄, 5 mM NaHCO₃, 150 mM KCl, 2 mM MgSO₄, 1 mM TCEP, 100 mM Tris-HCl buffer at pH 7.5), and were pre-incubated at 37°C for 15 min. Enzyme reaction was started by addition of 0.3 mM GTP substrate and stopped by addition of malachite green solution (3% ammonium molybdate, 3.46 mM malachite green, 2.5 M sulfuric acid). Rate of phosphate release was measured by absorbance at 630 nm. The IC₅₀ values were determined by fitting the data to a 2-parameters logistic model.

TABLE I. Ligands selected for *in-vitro* enzyme assay

Com- pound No.	ZINC ID	Com- pound No.	ZINC ID	Com- pound No.	ZINC ID
1	ZINC08449002	26	ZINC02162718	51	ZINC13807353
2	ZINC08439400	27	ZINC08443800	52	ZINC00648688
3	ZINC08453762	28	ZINC08437875	53	ZINC08398604
4	ZINC08456291	29	ZINC08441228	54	ZINC19923341
5	ZINC04577554	30	ZINC02189737	55	ZINC20219862
6	ZINC08427581	31	ZINC08383771	56	ZINC20219859
7	ZINC08492481	32	ZINC05918826	57	ZINC02133508
8	ZINC08396600	33	ZINC04065337	58	ZINC20219389
9	ZINC08425959	34	ZINC01811794	59	ZINC08453144
10	ZINC08386335	35	ZINC08440845	60	ZINC02860696
11	ZINC08431251	36	ZINC08449015	61	ZINC16228240
12	ZINC08400008	37	ZINC00702974	62	ZINC13571381
13	ZINC08398283	38	ZINC06195955	63	ZINC09096557
14	ZINC08492375	39	ZINC08383742	64	ZINC08425693
15	ZINC08451538	40	ZINC19938372	65	ZINC19938388
16	ZINC08452640	41	ZINC08426112	66	ZINC05360685
17	ZINC08424865	42	ZINC08438744	67	ZINC08695208
18	ZINC08417256	43	ZINC48696926	68	ZINC00657433
19	ZINC08383253	44	ZINC19938425	69	ZINC00863679
20	ZINC08426140	45	ZINC04061246	70	ZINC13945995
21	ZINC06197239	46	ZINC19938462	71	ZINC04664681
22	ZINC08454888	47	ZINC00623301	72	ZINC19872272
23	ZINC08401405	48	ZINC19923356	73	ZINC04114176
24	ZINC02049630	49	ZINC20264072		
25	ZINC08452470	50	ZINC19909927		

Effect of ligands on the survival of *H pylori* in acid medium

The acid resistance test was used to test the effect of selected UreG inhibitors on the survival of *H pylori* in acid medium.¹ In brief, *H pylori* SS1 strain was cultured in 3 mL Brucella broth (Becton, Dickinson & Co.) with 5% foetal bovine serum (Gibco) with or without 100 µM ligands in a microaerobic environment at 37°C for 2 days. 0.5 mL of *H pylori* culture at OD600 = 1 was centrifuged at 2000 g for 10 min and the cell pellet was then resuspended in pH 1 acid saline (100 mM HCl, 50 mM NaCl, 100 µM NiCl₂) with or without 5 mM urea and 100 µM ligands. After incubation at 37°C for 30 min, the survived colonies of *H pylori* were grown in BBL agar plates and were counted.

Results

Structure-based screening of UreG inhibitors and *in-vitro* enzyme assay

We have previously reported the crystal structure of UreG/UreF/UreH complex. UreG, a GTPase essential for urease maturation, forms a dimer when in complex with GTP and nickel.² We argued that any ligands that can block the active-site of UreG or its dimerisation should inhibit the GTPase activity. To

this end, we have performed five independent docking simulations, ~270,000 ligands from the SPECS library of ZINC database were screened *in-silico*. Among the ligand candidates selected for *in-vitro* enzyme assay (Table 1), ligand 2, 4, 5, and 37 showed inhibitory effect with < 50% at 100 µM.

Analogues of ligand 37 showed improvement in inhibition against UreG activity

Among the ligands that showed inhibition towards UreG, we selected ligand 37 for further characterisation because (1) a number of structural analogues are available commercially in the SPECS library; and (2) its chemical/physical properties are in closer agreement with the drug-likeness predicted by the Lipinski's rule of five (M.W. <~500, hydrogen bond acceptor <5 and acceptors <10, LogP <5).³ We identified 9 analogues of ligand 37 that shared a common 'central rings' structural motif, but differed in the R1 and R2 groups (Fig). To test the effect of different R1/R2 groups to the inhibitory effect on UreG activity, we measured the relative activity of UreG in the presence of 0-250 µM of ligand 37 and its analogues, and compared their IC₅₀ values (Fig). Noteworthy substitution of R1 group in ligand 37a resulted in a compound that did not inhibit UreG activity, suggesting the imidazole group in R1 is important. The IC₅₀ for ligand 37 was 59±3 µM. Substitution of R2 group resulted in IC₅₀ values in ligand 37b to 37i ranging from 21 to 85 µM (Fig). It is likely that ligand forms specific interaction with UreG, which is dependent on the chemical structure of R2. In particular, the best analogue, 37e, has a >2-fold decrease in the IC₅₀ values.

UreG inhibitors suppressed the survival of *H pylori* in acid medium

The best two inhibitors of UreG, 37e and 37h, were tested to determine if they affected the urease-dependent survival of *H pylori* in acid medium using an established method.¹ Consistent with previous observations, in the presence of 5 mM urea, *H pylori* survived in pH 1 for 30 min (Table 2). In contrast, survival of *H pylori* was greatly reduced when 100 µM of acetohydroxamic acid was added or when urea was absence. These observations suggest that the survival of *H pylori* in acid medium depends on the urease activity (Table 2). Interestingly, the survival of *H pylori* was suppressed to a level comparable to that in the absence of urea when 100 µM of UreG inhibitors 37e or 37h were added (Table 2). Taken together, our results suggest that these UreG inhibitors suppressed the survival of *H pylori* by abolishing the biosynthesis of active urease.

Discussion

In this study, we have performed structure-based screening to identify inhibitors of UreG. Based on the crystal structures determined in our laboratory, ~270000 ligands in the SPECS library of the ZINC

database were screened using the DOCK (<http://dock.compbio.ucsf.edu>), and 73 top ranked ligands were selected to assay experimentally for their inhibition against UreG. After improvement by screening structural analogues, the best UreG inhibitors have IC₅₀ values in the range of 20-30 μM.

Survival of *H pylori* in acidic environment is dependent on the urease activity that releases the neutralising ammonia from urea. *H pylori* cannot survive in acid medium without the substrate urea or in the presence of a urease inhibitor (Table 2).¹ Since the biosynthesis of active urease requires the GTPase activity of UreG, we anticipated that inhibitors of UreG should reduce the survivability of *H pylori* in acid medium. In fact, inhibitors 37e and 37h suppressed the survival of *H pylori* in acid medium (Table 2). The result is encouraging because blocking the biosynthesis of active urease can kill *H pylori* in acid medium, like what was observed for the urease inhibitor acetohydroxamic acid (Table 2).¹ Moreover, the growth of *H pylori* at neutral pH was not affected by these ligands. Taken together, our results suggest that the inhibition of *H pylori* growth in acid medium was a result of blocking the urease maturation pathway.

We have identified UreG inhibitors that can kill *H pylori* in acid medium. This suggests that blocking the urease maturation could be a novel target for *H pylori* infection. Nonetheless, there is still a long research/development process before any drugs of this kind are demonstrated clinically useful. UreG inhibitors 37e and 37h were tested for their *in-vivo* efficacy in an *H pylori*-infected mouse model.⁴ Only 1/10 in the 37h-treatment group showed negative results on the urease test. Although histological examination revealed a somewhat reduced infection of *H pylori* in the mouse stomach, the pathogen was not eradicated by the treatment of 37e or 37h. This result suggests that the inhibitors identified in this study still need further optimisation. One can use combinatorial chemistry or structure-based rational design to further improve the existing inhibitors of UreG. Another feasible strategy to improve efficacy is to combine the UreG inhibitors with urease inhibitors in the treatment of *H pylori*. Using a weak urease inhibitor such as acetohydroxamic acid in treating *H pylori* infection probably requires a high dose that may lead to other side-effects.⁵ We argue that UreG inhibitors should work synergistically with urease inhibitors because the required dose of urease inhibitors could be lower because the pathogen can no longer produce large amounts of active urease.

Funding

This study was supported by the Health and Medical Research Fund, Food and Health Bureau, Hong Kong SAR Government (#13120122). The full report is available from the Health and Medical Research Fund website (<https://rfs1.fhb.gov.hk/index.html>).

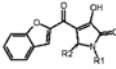
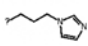
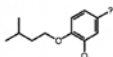
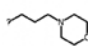
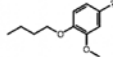

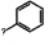

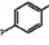

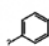
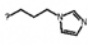
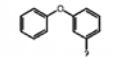

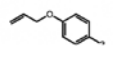

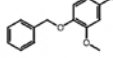

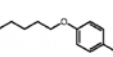

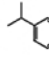
	ZINC ID	Central Rings	R1	R2	IC ₅₀ (μM)
37	ZINC00702974				59±3
37a	ZINC08441340				>250
37b	ZINC08897821				85±3
37c	ZINC04019664				54±4
37d	ZINC00702964				85±4
37e	ZINC00702966				21±2
37f	ZINC08441292				57±3
37g	ZINC08441299				34±2
37h	ZINC08441301				31±2
37i	ZINC00702980				39±2

FIG. IC₅₀ values of ligand 37 and its analogues (37a – 37i) in inhibiting GTPase activity of UreG

TABLE 2. Survival of *Helicobacter pylori* in acid medium is suppressed by UreG inhibitors

Treatment	Mean±SD colony count after acid shock, 10 ³ cfu/mL	Survival rate, %
-Urea	0.2±0.2	0.2
+Urea	117±11	100
+Urea +AHA	1.1±1.4	1.2
+Urea +ligand 37e	0.4±0.2	0.3
+Urea +ligand 37h	0.0±0.1	0.0

References

- Mooney C, Munster DJ, Bagshaw PF, Allardyce RA. *Helicobacter pylori* acid resistance. *Lancet* 1990;335:1232.
- Fong YH, Wong HC, Yuen MH, Lau PH, Chen YW, Wong KB. Structure of UreG/UreF/UreH complex reveals how urease accessory proteins facilitate maturation of *Helicobacter pylori* urease. *PLoS Biol* 2013;11:e1001678.
- Lipinski CA, Lombardo F, Dominy BW, Feeney PJ. Experimental and computational approaches to estimate solubility and permeability in drug discovery and development settings. *Adv Drug Deliv Rev* 2001;46:3-26.
- Aristoteli LP, O'Rourke JL, Danon S, et al. Urea, fluorofamide, and omeprazole treatments alter *Helicobacter* colonization in the mouse gastric mucosa. *Helicobacter* 2006;11:460-8.
- Follmer C. Ureases as a target for the treatment of gastric and urinary infections. *J Clin Pathol* 2010;63:424-30.

Role of HP1076 in type IV secretion pathway in *Helicobacter pylori*: abridged secondary publication

WL Lam, M Li, KF Lau, VSF Chan, SWN Au *

KEY MESSAGES

1. *Helicobacter pylori* HP1076 is essential for translocation and phosphorylation of CagA.
2. Deletion of HP1076 inhibits transcription of CagD and also affects the assembly of Cag T4SS components CagT and CagM.
3. It is likely that the effects of HP1076 on cag T4SS assembly and activity are mediated by down-regulation of CagD.

Hong Kong Med J 2020;26(Suppl 4):S32-4

HMRP project number: 13120022

¹ WL Lam, ² M Li, ¹ KF Lau, ² VSF Chan, ¹ SWN Au

¹ School of Life Sciences, The Chinese University of Hong Kong, Hong Kong

² Department of Medicine, The University of Hong Kong, Hong Kong

* Principal applicant and corresponding author: shannon-au@cuhk.edu.hk

Introduction

Helicobacter pylori infection is recognised as a primary risk factor for gastric adenocarcinoma and gastric lymphoma.¹ Strains of *H pylori* harbouring cag pathogenicity island (PAI) are typically associated with a higher rate of disease.² Cag PAI encodes about 27 proteins, some of which comprise a type IV secretion system (T4SS) for the translocation of CagA effector into gastric epithelial cells. Upon translocation, CagA interacts with various host cell proteins, resulting in abnormal proliferation, deregulation of cell-cell contacts and induction of proinflammatory cytokines. Little is known about the structural organisation of T4SS and the mechanistic details of CagA translocation. Notably, nine cag PAI genes essential for CagA delivery are unique in *H pylori*, suggesting that cag T4SS in *H pylori* differs considerably from T4SSs in other bacterial species.

This study focuses on the functional role of an uncharacterised protein HP1076 in cag T4SS. HP1076 is reported to be a co-chaperone of flagellar export chaperone FliS.³ Interestingly, HP1076-null mutant has no significant effect on flagella synthesis and bacterial motility (unpublished data). Rather, our data show that translocation and phosphorylation of CagA is reduced in gastric epithelial cells infected with HP1076-null mutant. We therefore hypothesise that HP1076 may involve in the other secretory pathways, in particular cag T4SS.

Methods

We obtained a collection of 25 Cag antibodies using purified recombinant proteins and commercially synthesised peptides for immunisation. We characterised the expression of Cag proteins, CagA translocation and phosphorylation by

immunoblotting upon different infection dosages. In addition, assembly of T4SS was studied by limited proteolysis. Attempts to isolate potential relay proteins of HP1076 were carried out by pull-down assays and 2-D gel electrophoresis.

Results

Cloning, expression and antibody production of Cag T4SS proteins

In this study, all 27 genes for T4SS from *H pylori* were successfully cloned into *E coli* expression vector. Expression and purification of individual Cag proteins were also tested and optimised. Currently, a total of 11 recombinant Cag proteins including Cag3, Cag5, VirB11-like cag protein, CagZ, Cag10, CagX, CagT, CagS, CagM, CagF, CagD were purified for immunisation for polyclonal antibody production. Some of the cag proteins including Cag1, Cag2, Cag4, CagW, CagV, CagU, CagQ, CagN, CagL, CagI, CagH, CagG, CagE, CagC, CagB could not be purified in sufficient quantity for immunisation. Antibodies against these Cag proteins were raised using synthetic peptides.

Characterisation of Cag T4SS protein expression level in wild-type strain and HP1076-null mutant

To determine whether HP1076 is linked to the biosynthesis of cag T4SS, expression levels of Cag proteins were analysed by immunoblotting. Our results show that expression levels of cag proteins between G27 wild-type strain and HP1076-null mutant were comparable, with an exception of CagD, which was completely undetectable in HP1076-null mutant.

Since HP1076 possess co-chaperone activity

towards FliS,³ we questioned whether HP1076 had a stabilising effect on CagD, preventing it from degradation. Our result showed that there was no direct biophysical contact between HP1076 and CagD, suggesting that the down-regulation of CagD in *HP1076*-null mutant was likely at transcription level. Transcription inactivation of CagD was further confirmed by real-time PCR, that the mRNA level of CagD was reduced by about 70%.

Characterisation of Cag T4SS assembling by limited proteolysis

We further characterised the effect of HP1076 on T4SS assembly by trypsin-limited proteolysis. For T4SS surface exposed proteins, they are accessible to proteolytic attack; therefore, comparison of the trypsin digestion pattern will allow us to probe for any changes in T4SS maturation and assembly. Our results show that the digestion profiles of CagI, CagT and CagX from the G27 strain and *HP1076*-null mutant were comparable; however, it appears that CagI in *HP1076*-null mutant were slightly resistant to proteolysis. Significant differences of digestion patterns were revealed when cells were first treated with osmotic shock that the bacterial outer membrane was permeabilised before proteolysis. Specifically, CagT in *HP1076*-null mutant was completely digested in small quantity of trypsin. CagM in *HP1076*-null mutant was also shown to be more susceptible to trypsin digestion, though the extent was less severe when compared to CagT. Taken together, these results suggested that deletion of HP1076 interrupted the assembly of T4SS.

Characterisation of CagA phosphorylation and IL-8 production in infected AGS cells

We next evaluated the functional importance of HP1076 and its association with T4SS in bacterial infection, translocation and phosphorylation of CagA in host cells were examined. At early phase of infection, gastric epithelial cells infected with *HP1076*-null mutant showed a lower level of translocated CagA. After 2 hours of infection, there was no significant difference in CagA level between cells infected with G27 strain and *HP1076*-null mutant. Noteworthy, phosphorylation of CagA was almost completely suppressed in cells were infected with *HP1076*-null mutant. These results suggested that effective translocation and phosphorylation of CagA was HP1076 dependent. Additionally, *HP1076*-null mutant led to a reduction of IL-8 secretion that may link to inhibition of CagA phosphorylation.

Isolation of HP1076 interacting partners in *H pylori* and AGS cells by pull-down assays

To understand the mechanistic details of HP1076 on T4SS, and CagA secretion and phosphorylation, we applied pull-down assays to isolate potential

interacting partner of HP1076 in *H pylori* lysate and gastric epithelia cells. However, no extra band was detected.

Additionally, protein profiling of *H pylori* G27 strain and *HP1076*-null mutant were analysed by 2D-PAGE. Down-regulation of 9 proteins involved in amino acid metabolism and protein synthesis, and up-regulation of 6 proteins involved in antioxidant defence mechanism were found in *HP1076*-null mutant.

Discussion

Disease outcomes of *H pylori* infection are tightly associated with bacterial strains that possess cag pathogenicity island, which encodes protein components of a T4SS, an effector protein CagA and various proteins that are unique but with unknown function in *H pylori*. Our research team has previously found that *HP1076* knockout strain had a reduced secretion of CagA to gastric epithelial cells (unpublished data). Since secretion of cagA is fully dependent on cag T4SS, we hypothesised that *HP1076* may be involved in T4SS. In the present study, we successfully obtained a repertoire of Cag antibodies using purified recombinant proteins and commercially synthesised peptides. Deletion of *HP1076* led to transcription inactivation of CagD. CagD has been reported to be essential for CagA translocation.⁴ It is unclear whether the inhibitory effect of *HP1076* on CagA secretion is a direct mechanism or indirectly mediated through down-regulation of CagD. Since the crystal structure of *HP1076* does not display any positively charged groove for nucleotide binding,³ we speculate that *HP1076* may inactivate the transcription of CagD via unidentified role.

In general, cag PAI encodes numerous protein orthologues of VirB/VirD4 system that the two T4SS may share similar core structure. However, little is known about T4SS that secrete effector proteins, especially cag T4SS. Recently study has isolated the membrane spanning core complex of cag T4SS which is composed of CagM, CagT, Cag3, CagX and CagY,⁵ among which CagM, CagT and Cag3 are unique to *H pylori*. Here, our results from limited proteolysis indicated that *HP1076* may interfere the structural assembly of cag T4SS, especially CagT and CagM. Since both Cag proteins are key structural components required for T4SS activity,⁵ it implies that the reduction of CagA translocation in *HP1076*-null mutant may also be due to defect in T4SS assembly, in addition to the down-regulation of CagD.

Our study further demonstrated that deletion of *HP1076* not only suppressed CagA translocation. Interestingly, tyrosine-phosphorylation of CagA was severely inhibited. CagA phosphorylation is catalysed by Src family protein kinases and c-Abl

kinase. Taken together with the results from the pull-down assays, it is unlikely that the HP1076 directly binds on the two kinases and inhibits their CagA phosphorylation activity. A previous genetic study showed that CagD is necessary for both translocation and phosphorylation of CagA,⁴ we speculate that the reduced CagA phosphorylation is mediated through down-regulation of CagD induced by HP1076 knockout. In contrast, though CagD is associated with the maximal IL-8 release,⁴ our results did not reveal any difference in IL-8 secretion between wild type G27 strain and HP1076-null mutant.

Collectively, our results suggest that HP1076 is necessary for cag T4SS activity, especially CagD expression. Since CagD can be found as a secreted protein, cytosolic protein and inner membrane protein, it may play a multifunctional role in T4SS. Probably, the effects of HP1076 on T4SS assembly, and CagA translocation and phosphorylation are primary due to the inactivation of CagD gene expression, though direct function of HP1076 on T4SS cannot be eliminated and needs further investigation. We attempted to isolate interacting partner of HP1076 in both gastric epithelial cells and *H pylori*, however no stable complex can be obtained. Comparison of protein profiling between the G27 strain and HP1076 revealed various differentially expressed proteins. Yet, none of them have been linked to T4SS that further in-depth studies are required in the future. In conclusion, the present study provides an example to demonstrate the regulation of T4SS beyond the cag pathogenicity island.

Acknowledgement

We thank Jacinth Li for her technical help in protein purification. We also thank Prof Vera Chan of The University of Hong Kong for the gene expression analysis.

Funding

This study was supported by the Health and Medical Research Fund, Food and Health Bureau, Hong Kong SAR Government (#13120022). The full report is available from the Health and Medical Research Fund website (<https://rfs1.fhb.gov.hk/index.html>).

References

1. Marshall BJ. Virulence and pathogenicity of *Helicobacter pylori*. *J Gastroenterol Hepatol* 1991;6:121-24.
2. Fischer W, Puls J, Buhrdorf R, Gebert B, Odenbreit S, Haas R. Systematic mutagenesis of the *Helicobacter pylori* cag pathogenicity island: essential genes for CagA translocation in host cells and induction of interleukin-8. *Mol Microbiol* 2001;42:1337-48.
3. Lam WW, Woo EJ, Kotaka M, et al. Molecular interaction of flagellar export chaperone FliS and cochaperone HP1076 in *Helicobacter pylori*. *FASEB J* 2010;24:4020-32.
4. Cendron L, Couturier M, Angelini A, Barison N, Stein M, Zanotti G. The *Helicobacter pylori* CagD (HP0545, Cag24) protein is essential for CagA translocation and maximal induction of interleukin-8 secretion. *J Mol Biol* 2009;386:204-17.
5. Frick-Cheng AE, Pyburn TM, Voss BJ, McDonald WH, Ohi MD, Cover TL. Molecular and structural analysis of the *Helicobacter pylori* cag type IV secretion system core complex. *MBio* 2016;7:e02001.

Characterisation of *Staphylococcus aureus* virulence factor EsxA and structure-based screening of EsxA inhibitors for combating methicillin-resistant *S aureus*: abridged secondary publication

KH Sze, RYT Kao *

KEY MESSAGES

1. EsxB did not interact with EsxA by cell-free assays (ITC and NMR titration) and cell-based assays (coIP and pull-down).
2. Pull-down and NMR titration assays showed that EsxA was interacting with lipid mediators HOTrE and sphingosylphosphorylcholine, respectively. These results suggested that EsxA may function as a lipid mediator binding protein, and that EsxA is an immune evasion gene and provide important clue to delineate its mechanism of immune evasion.
3. A high performance platform was established for *in silico* structure-based screening against pathogen targets. The EsxA X-ray structure was subjected to structure-based screening with a ligand library containing 6.8 million lead-like or

active lead ligands.

4. Of the 100 highest-scoring compounds, five were validated by the secondary NMR titration screen. One hit compound (6058448) showed MIC at 25 μ M level by broth microdilution test, and another hit compound (5674203) also showed antivirulence effects by inhibiting the expression of both protein A and alpha-toxin of US300 strain.

Hong Kong Med J 2020;26(Suppl 4):S35-8
HMRF project number: 13120862

KH Sze, RYT Kao

Department of Microbiology, The University of Hong Kong, Hong Kong

* Principal applicant and corresponding author: khsze@hku.hk

Introduction

Staphylococcus aureus is a highly adaptive Gram-positive bacterium and commensal of the human skin and nostrils. *S aureus* is a common cause of minor skin and wound infections, but it can also cause serious and even fatal infections, particularly in immunocompromised persons. Methicillin-resistant *S aureus* (MRSA) infection is an alarming threat, leading to life-threatening diseases such as endocarditis, pneumonia, and toxic shock syndrome.¹ MRSA has been endemic in Hong Kong since mid-1980s. Approximately 70% and 58% of the total and blood culture isolates of *S aureus* in Hong Kong public hospitals are MRSA, respectively. There is a need to develop new approaches and druggable targets for combating MRSA.

S aureus pathogenesis depends on a specialised protein secretion system (type VII-like Ess) that delivers a range of virulence factors to assist infectivity by establishment of abscess lesions and suppression of host immune responses. EsxA and EsxB are two of the confirmed virulence factors excreted by *S aureus*.² EsxA is reported to be an immune evasion gene but how it can achieve

this function remains unclear.³ EsxA and EsxB are small α -helical polypeptides belonging to a family of WXG100 motif proteins, which have a size of approximately 100 amino acids containing a helical structure and a conserved Trp-Xaa-Gly (WXG) motif. ESAT-6 (homologue of *S aureus* EsxA) and CFP-10 (homologue of *S aureus* EsxB), secreted as a heterodimer by *Mycobacterium tuberculosis*, are the founding members of the WXG100 motif family. Both proteins are crucial for the replication of *M tuberculosis* in macrophages and presumably also for the pathogen's ability to suppress innate and adaptive immune responses. Mutants that failed to secrete EsxA and EsxB displayed defects in the pathogenesis of *S aureus* murine abscesses, suggesting that these specialised secreted WXG100 motif proteins may be a general strategy of human bacterial pathogenesis.² Therefore, EsxA and EsxB are promising drug targets for combating MRSA and may have add-on implications in fighting against other drug-resistant pathogens such as multidrug-resistant strains of *M tuberculosis*.

A homodimeric structure of EsxA has a four-helix bundle fold.⁴ The structures of EsxB and the

putative EsxA-EsxB complex remain unknown. The actual role of EsxA and molecular basis for its function remain unclear. The expectation that EsxA will be secreted by forming a heterodimer with EsxB in analogy with the well-characterised ESAT-6/CFP-10 heterodimeric complex in *M tuberculosis* is also illusive. Therefore, characterisation of the binding of *S aureus* EsxA with EsxB and identification of other EsxA interacting partners or small substrates will provide important information in understanding the functional role of EsxA.

This pilot study aims to characterise the interaction of *S aureus* EsxA with EsxB by cell-based and cell-free methods and to perform *in silico* structure-based screening to identify inhibitors of EsxA for combating MRSA.

Methods and Results

Virulence factors EsxA and EsxB of *S aureus* were cloned, and their labelled and unlabelled His-tagged

recombinant protein samples were produced for cell-free and cell-based interaction studies.

The backbone resonance assignments of EsxA were completed using a series of 3D triple resonance NMR experiments to allow performing interaction studies of labelled EsxA with small ligand hit compounds, lipid molecules and EsxB using NMR chemical shift perturbation titration method.

Cell-free titration assays including ITC and NMR indicated that no *in vitro* interaction between the recombinant EsxA and EsxB samples (Fig 1). Cell-based coIP of EsxA against US300 infected J774 macrophages and pull-down assays of EsxA indicated that EsxB was not directly binding with EsxA. Instead, a lipid mediator molecule HOTrE was found in the pull-down extract of EsxA, indicating EsxA may be a lipid-binding protein. Subsequent *in vitro* NMR titration assay indicated that another lipid mediator, sphingosylphosphorylcholine, could also bind to EsxA. These results support that EsxA is a lipid-binding protein.

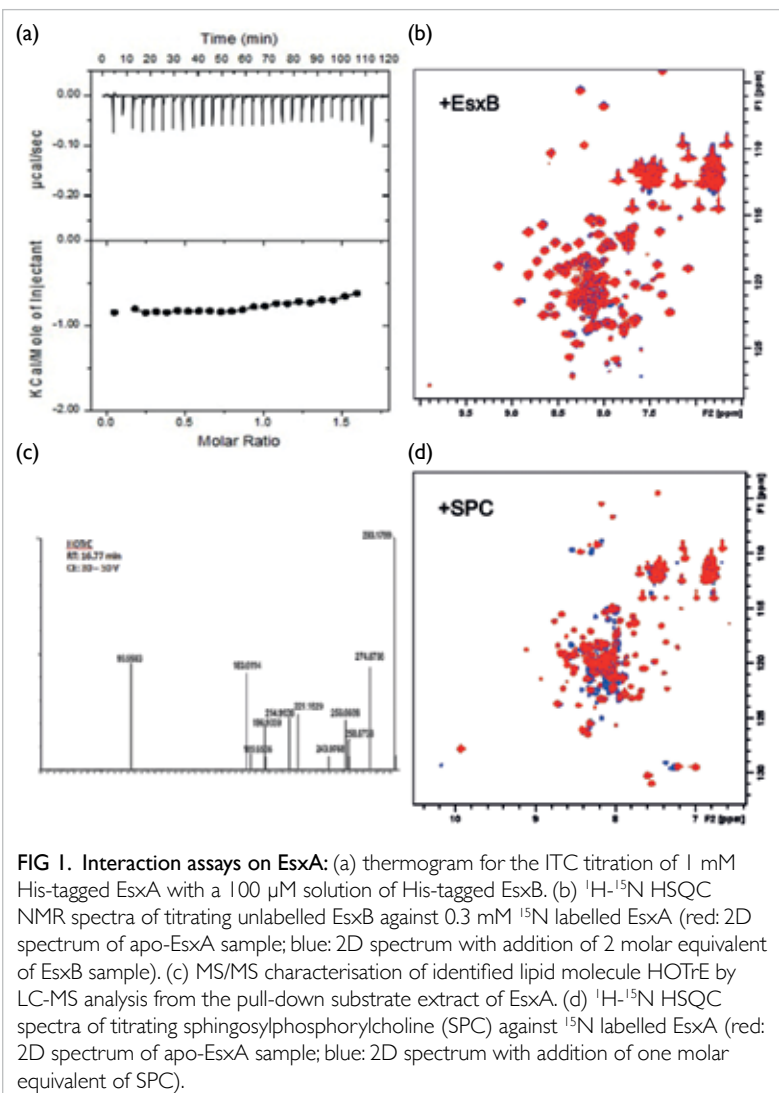
Two dedicated Dell OptiPlex 9020 workstation computers with Intel Core i7-4770 Quad Core Processor and 32GB Ram were setup with Fedora 15 Linux operating system and all required software for running Autodock/Vina program. These workstations have established a dedicate research platform and the capacity for performing *in silico* structure-based screening on a target protein. A compound library containing 6746897 Lead-Like compounds from ZINC database and 50240 compounds from active lead library of ChemBridge Corp was setup for the screening.

Autodock/Vina dockings were completed on all 6.8 million ligands in the library against the X-ray structure 2V50 of EsxA. Scoring sorting and clustering analysis by AuPosSOM of the best-hit ligands according to their structural features were performed in order to draw up the list of best docking scoring ligands for *in vivo* validation and testing. Fig 2 shows the AuPosSOM scoring plots and the graphical representation of the major predicted contacts.

Of the 100 highest-scoring compounds, five produced significant cross-peak movements or intensity variations upon titration into ^{15}N labelled EsxA in secondary experiment screen of NMR titration assay.

The broth microdilution test showed that hit compound 6058448 showed MIC at 25 μM , whereas hit compounds 5224045, 5546503, and 6238413 have MIC >100 μM .

Hit compound 5674203 showed significant antivirulence effects by inhibiting the expression of both protein A and alpha-toxin, whereas hit compounds 5224045, 5546503, 6058448, and 6238413 did not show any inhibitory effects (data not shown).



ITC experiment has been performed using recombinant EsxA and the validated hit compound 5674203 with antivirulence activity. The thermogram was best fitted with one-site model to generate a binding affinity K_d value of $90.0 \mu\text{M}$, $N=0.5$, $\Delta H=-59.6 \text{ kcal/mol}$, $\Delta S=-186 \text{ cal/mol/deg}$.

Discussion

EsxB did not interact with EsxA. Instead, EsxA was shown to be a lipid mediator binding protein. EsxA is a secreted virulence factor by *S aureus* implicated to be an immune evasion gene, but its mechanism of immune evasion remains unknown.³ The ability of EsxA to trap lipid mediators may provide clues about its immune evasion function. We have reported that a highly secreted and helical virulence factor Mp1p of fungal pathogen, *Talaromyces marneffeii*, binds and sequesters a key proinflammatory lipid (arachidonic acid) to dampen host innate immune response.⁵ Therefore, bacterial pathogens may have a similar host immune evasion mechanism. The function for the highly secreted and helical WXG100 motif virulence factor proteins found in many bacterial species remains unclear. It is of interest to investigate whether other WXG100 motif virulence factors also serve as lipid-binding proteins to evade host immune defence. Our preliminary NMR titration data obtained on the heterodimeric WXG100 motif ESAT-6/CFP-10 of TB showed that it is also able to bind sphingosylphosphorylcholine.

We have established a dedicated Linux computer platform for *in silico* structure-based screening for drug targets with known high-resolution structures. MRSA is of great concern because it is quickly acquiring resistance to all clinical antibacterial agents. There is an urgent need to develop new approaches and new druggable targets to combat MRSA with lower chances of developing drug resistance. In this study, we identified several hit compounds against MRSA through *in silico* structured-based screening against the novel target EsxA of *S aureus*. These hit compounds likely act against MRSA through a mechanism different from the existing antibiotics, because EsxA is a virulence factor of *S aureus*. For example, hit compound 5674203 showed no antibacterial effect but significant antivirulence effects to enhance host cell protection. Antivirulence drug against *S aureus* infection with diminished virulence will cause less or no damage to the host cells and tissues and will not subject to natural selection pressure so that the antivirulence drug is less likely to cause drug resistance. Through the hit-to-lead process, these hit compounds can be further modified and improved to attain higher potency and better pharmacokinetics properties. The improved compounds could be the candidates for new drug development against MRSA.

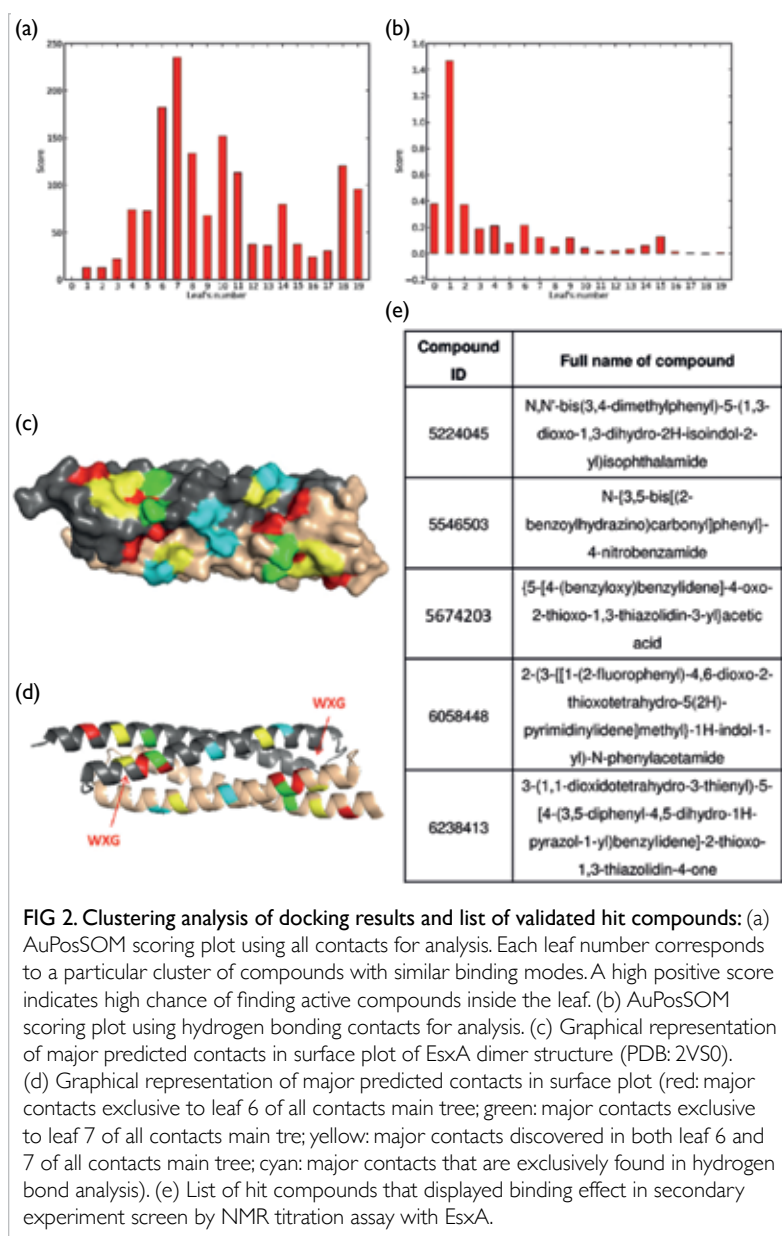


FIG 2. Clustering analysis of docking results and list of validated hit compounds: (a) AuPosSOM scoring plot using all contacts for analysis. Each leaf number corresponds to a particular cluster of compounds with similar binding modes. A high positive score indicates high chance of finding active compounds inside the leaf. (b) AuPosSOM scoring plot using hydrogen bonding contacts for analysis. (c) Graphical representation of major predicted contacts in surface plot of EsxA dimer structure (PDB: 2V50). (d) Graphical representation of major predicted contacts in surface plot (red: major contacts exclusive to leaf 6 of all contacts main tree; green: major contacts exclusive to leaf 7 of all contacts main tree; yellow: major contacts discovered in both leaf 6 and 7 of all contacts main tree; cyan: major contacts that are exclusively found in hydrogen bond analysis). (e) List of hit compounds that displayed binding effect in secondary experiment screen by NMR titration assay with EsxA.

Acknowledgement

We thank Prof KY Yuen for providing the *S aureus* strains and Dr JD Huang for providing the EsxA antibody used in the IP experiment.

Funding

This study was supported by the Health and Medical Research Fund, Food and Health Bureau, Hong Kong SAR Government (#13120862). The full report is available from the Health and Medical Research Fund website (<https://rfs1.fhb.gov.hk/index.html>).

References

1. Grundmann H, Aires-de-Sousa M, Boyce J, Tiemersma E. Emergence and resurgence of meticillin-resistant *Staphylococcus aureus* as a public-health threat. *Lancet* 2006;368:874-85.
2. Burts ML, Williams WA, DeBord K, Missiakas DM. EsxA and EsxB are secreted by an ESAT-6-like system that is required for the pathogenesis of *Staphylococcus aureus* infections. *Proc Natl Acad Sci U S A* 2005;102:1169-74.
3. McCarthy AJ, Lindsay JA. Genetic variation in *Staphylococcus aureus* surface and immune evasion genes is lineage associated: implications for vaccine design and host-pathogen interactions. *BMC Microbiol* 2010;10:173.
4. Sundaramoorthy R, Fyfe PK, Hunter WN. Structure of *Staphylococcus aureus* EsxA suggests a contribution to virulence by action as a transport chaperone and/or adaptor protein. *J Mol Biol* 2008;383:603-14.
5. Sze KH, Lam WH, Zhang H, et al. *Talaromyces marneffei* Mp1p is a virulence factor that binds and sequesters a key proinflammatory lipid to dampen host innate immune response. *Cell Chem Biol* 2017;24:182-94.

Genomic and transcriptomic analyses of the *Salmonella* virulence regulatory network: abridged secondary publication

MHY Wong, D Lin, R Li, EWC Chan, S Chen *

KEY MESSAGES

1. The virulence of *Salmonella* is not defined by the genetic traits of specific strains but by the expression of specific house-keeping and stress-response genes, including HilA, HilD, HilC, and RNase III.
2. *Salmonella* double-stranded RNA (dsRNA) can induce host immune responses.
3. The RNase III level defines the ability of a *Salmonella* strain to trigger host immune response.
4. Over-expression of RNase III occurs in the highly

virulent strains *Salmonella*, resulting in a lower dsRNA level and hence milder immune response and higher virulence.

Hong Kong Med J 2020;26(Suppl 4):S39-42
HMRF project number: 13121412

MHY Wong, D Lin, R Li, EWC Chan, S Chen

Department of Applied Biology and Chemical Technology, The Hong Kong Polytechnic University, Hong Kong

* Principal applicant and corresponding author: sheng.chen@polyu.edu.hk

Introduction

To infect, bacteria must replicate and produce a complex array of gene products for invasion and survival in the host environment.^{1,2} Microorganisms frequently undergo adaptive physiological and genomic changes; bacterial virulence is subjected to constant regulatory pressure characteristic of the nature of environmental stress that the organisms encounter. *Salmonella* express a repertoire of known virulence factors and undergo physiological phase transition upon traversing between the natural environment and host body,¹⁻³ encountering and overcoming stresses of different nature. Our preliminary study indicated that strains of the same serotype often exhibit a spectrum of phenotypic characteristics such as survival fitness in macrophages. We hypothesise that *Salmonella* constantly generates mutational changes for environmental adaptation in such a way that only a subset of the environmental organisms is physiologically fit to infect humans. This study aimed at analysing the genetic backgrounds and gene expression profiles of organisms that exhibit high and low virulence potential under clinically relevant conditions. Findings can provide invaluable insight into the key regulatory and functional mechanisms that define the virulence level of *Salmonella*.

Methods

Salmonella enteritidis strains (30 clinical samples, 5 food samples, and 26 Centers for Disease Control and Prevention samples) were used in this study.

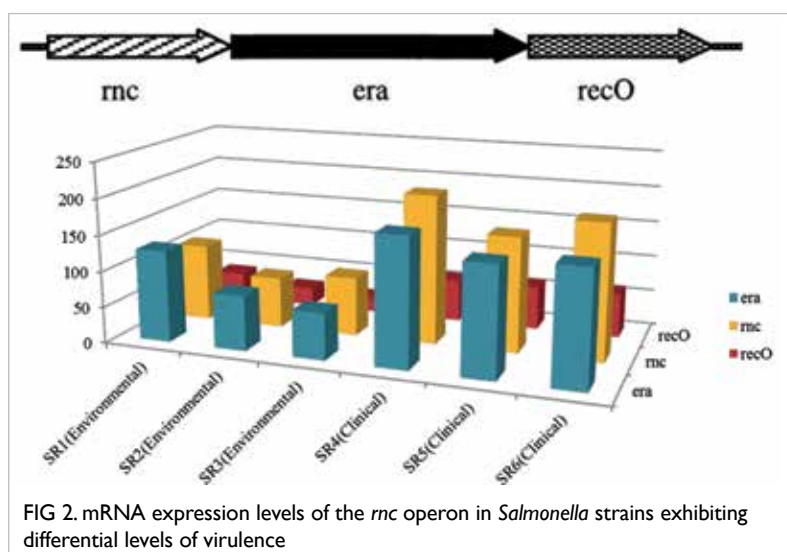
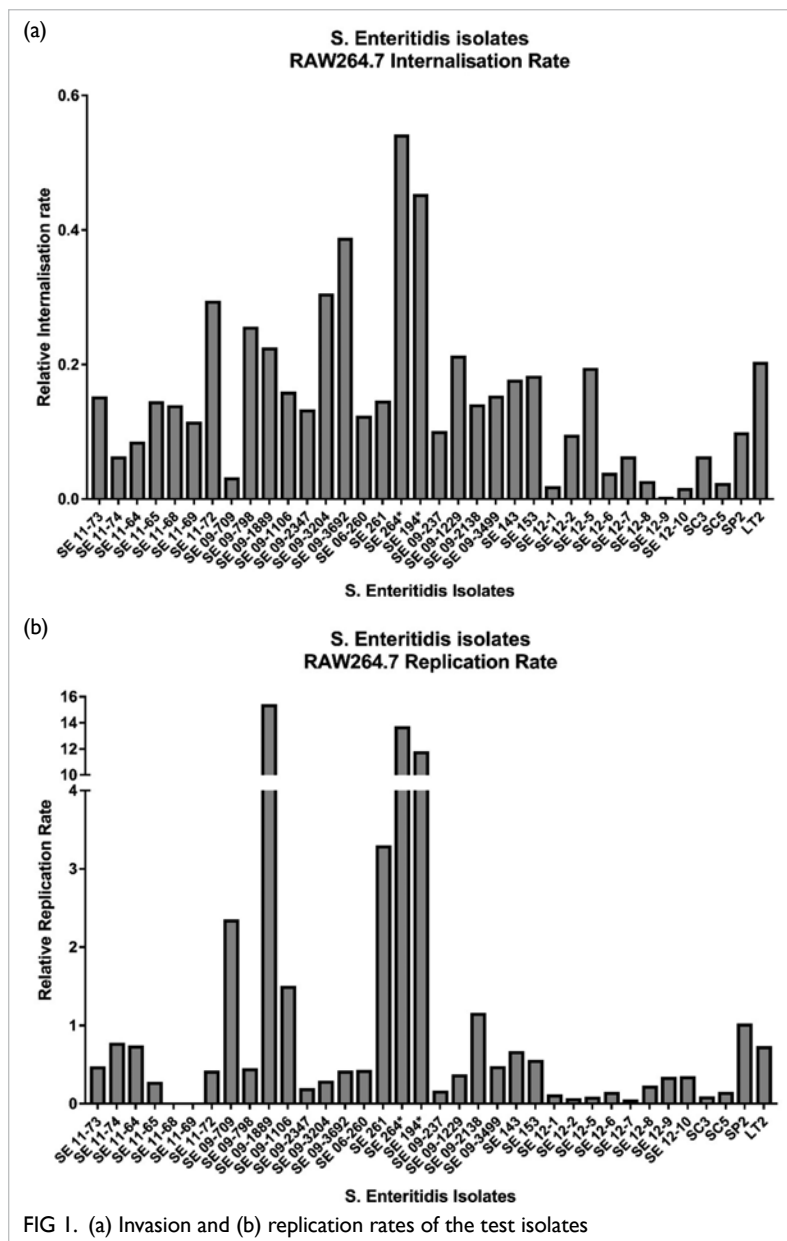
Salmonella typhimurium LT2 was used as a reference strain.

DNA was extracted from overnight culture of the test organisms using PureLink Genomic DNA Mini kit (Invitrogen) and used for PCR-virulotyping and whole genome sequencing. Eleven known virulence determinants were tested: *invA*, *avaR*, *ssaQ*, *mgtC*, *siiD*, *sopB*, *gipA*, *sodC*, *sopE*, *spvC*, and *bcfC*.

The virulence of *Salmonella* strains was characterised by infecting RAW 364.7 cells. Internalisation rate and replication rate were calculated as follows: 25 μ L of bacterial suspension were added to the wells at a multiplicity of infection of 10:1, followed by incubation at 37°C, 5% CO₂ for 25 minutes; the plates were then washed twice with pre-warmed PBS and incubated with media containing 100 μ g/mL gentamicin for 1 h. The supernatant was then removed at 2 and 16 h after infection; the cells were then washed twice with pre-warmed PBS and lysed with 0.1% Triton X-100. Serial dilutions of the lysates (10⁻¹, 10⁻², 10⁻³, 10⁻⁴) were then plated onto LB agar to enumerate the intracellular bacteria.

Invasion rate or internalisation rate (bacteria number to infect or intracellular CFU after 2 h per well after infection) was used to describe the invasion ability of isolates.⁴ Replication rate (intracellular CFU after 2 h or intracellular CFU per well after 16 h) of the test isolates was also recorded.

To detect the potential virulence related mutagenesis or emergence of novel virulence genes, whole genome sequencing of selected strains was conducted on the Illumina platform. To depict the



expression profiles of different virulence-related genes, transcriptome analysis of high and low virulence was performed. The strains were harvested in LB broth with 0.6 of OD600, and the total RNA was extracted using RNeasy Mini Kit and proceed to perform RNA-seq in BGI Company in Hong Kong.

To investigate the functions of genes, mutant strains were constructed using the RED-mediated recombination system reported.⁵

Overnight *Salmonella* cultures were diluted 100× in LB broth and cultured for 3 and 12 h at 37°C. The bacteria were collected, and total RNA was isolated by the RNA isolation kit (Qiagen). Bacterial total RNA was quantified, and similar amount of RNA was separated on agarose gel, transferred to PVDM membrane, and detected using J2 antibody.

RAW264.7 cell was cultured in DMEM. Overnight cell culture was transfected with total RNA with or without Lipo2000 transfection reagent based on the manufacturer instructions. The expression of different immune factors was measured by qRT-PCR.

Results

We first investigated if food and clinical isolates of *S. enteritidis* harboured different virulence gene profiles. Based on the prevalence of virulence-related genes in 61 *S. enteritidis* isolates, we did not observe significant difference in the distribution of virulence genes among these isolates, suggesting that *S. enteritidis* strains that originated from different sources exhibited a similar level of virulence.

We then examined if the strains exhibited differential virulence levels despite their similar genetic profiles. Strains of the highest and lowest virulence levels were determined by their invasion capability and survival rate in macrophages. We found that genetically identical strains may exhibit highly different virulence levels (Fig 1). The lowest and highest relative invasion rates of the test isolates were 0.0009 and 0.3863, respectively, a difference of >400 fold. For replication rate, the lowest and highest were 0.0348 and 15.3199, respectively.

To delineate the cellular basis of differential virulence levels observable in genetically identical organisms, strains exhibiting the lowest and highest virulence were subjected to RNA-Seq. The high virulence group of *S. enteritidis* consistently displayed higher levels of expression of virulence-related and host adaptation-related genes than the low virulence group. In particular, expression of specific two-component system (PhoQ), carbon storage regulator (CsrA), invasion protein regulator (HilA), DNA-binding protein Fis, *araC* family transcriptional regulator (HilD and HilC), RNase III and other elements with less definitive functions such as SicA were found to be dramatically increased in high virulence group but not in the low virulence group.

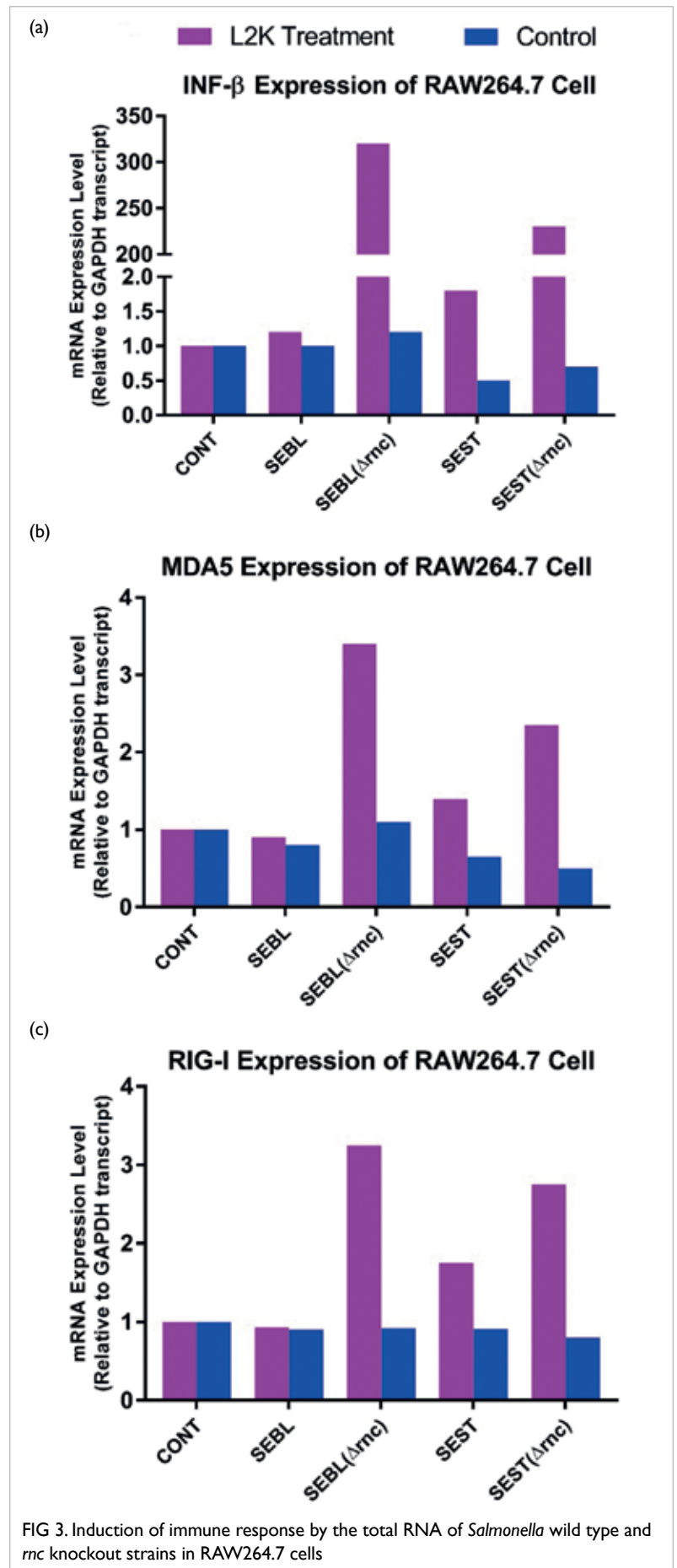
The *rnc* gene, which encodes RNase III, was also found to play a particularly important role in *Salmonella* virulence (Fig 2). In a mobility assay, two *rnc* knockout strains, S1:: Δrnc and S3:: Δrnc , were found to exhibit significantly reduced mobility, suggesting that *rnc* is essential for *Salmonella* mobility. In addition, deletion of the *rnc* gene also resulted in insignificant impairment of the virulence of *Salmonella* in a wax worm model, thus further confirming the important role of *rnc* in *Salmonella* virulence.

We then tested whether *Salmonella* strains S1 and S3 and the respective *rnc* knockout strains could induce immune response. The expression level of IFN- β increased with the increasing multiplicity of infection. In addition, *rnc* knockout strains were found to exhibit higher levels of expression of IFN- β , compared with the wild type S1 and S3 strains (Fig 3). We also tested whether the role of RNase III in inducing immune response is due to its ability to control formation of dsRNA in *Salmonella*. Double-strand RNA assay showed that dsRNAs were only detectable in S1:: Δrnc and S3:: Δrnc , but not in the wildtype strains, suggesting that RNase III indeed plays an important role in cleaving endogenous dsRNAs in *Salmonella*.

To check whether *Salmonella* dsRNA was involved in bacterial infection and host immune response, we performed dsRNA transfection assay in RAW264.7 cells. After 16 h transfection, bacterial RNA from *rnc* knockout strains, but not those of the wild type strains, caused over-expression of IFN- β . Induction of IFN- β may be mediated by the over-expression of RIG-I and MDA5 receptors, which were also inducible by *Salmonella* RNA. These findings suggest that bacterial RNAs could trigger the immune response.

Discussion

We presented an overview of the *Salmonella* virulence profile at both genetic and gene expression level and the underlying basis of high virulence in specific strains. The genetic and virulence gene profiles of all test strains of *S enteritidis* were highly similar, suggesting that any difference in virulence level between individual strains is not due to a discrepancy in the virulence gene profile. Nonetheless, virulence assays that tested the ability of *Salmonella* to invade and replicate in macrophages showed that the invasiveness of individual strains could differ significantly, despite their almost identical virulence gene profiles. The high-level virulence in *S enteritidis* was associated with up-regulation of many virulence-related and host adapted related genes, as well as a number of global regulators such as those encoding PhoQ, CsrA, HilA, and RNase III. These findings suggest that the pathogenicity of *Salmonella*, or perhaps



other bacterial pathogens, is highly dependent on the transcription status of a wide range of intrinsic regulatory and functional genes that are present in all strains. Such findings imply that acquisition of new virulence genes may only play a rather minor role in fine-tuning the basal virulence level of the organism.

Of particular importance is the *rnc* gene, which is known to encode RNase III and over-expressed in high virulence *Salmonella* strains. We elucidated the role of RNase III in regulating the host immune response, and hence, indirectly, survival of the pathogen in the host body. The *rnc* knockout strain was less virulent and exhibited lower mobility. *rnc* knockout strains indeed exhibited higher levels of expression of IFN- β . dsRNAs were only detectable in *rnc* knockout strains. Bacterial RNAs could be recognised by immune cells, triggering the immune response. Therefore, our data confirm that dsRNA is responsible for the induction of the host immune response and that RNase III plays a key role in regulating such induction potential. Over-expression of RNase III in *Salmonella* is expected to result in a lower dsRNA level, leading to a milder immune response inducible by *Salmonella*. These findings may help devise novel strategies to attenuate bacterial virulence by suppressing expression of specific house-keeping and stress response genes, as well as their ability to degrade dsRNA, a trigger of host immune response.

Funding

This study was supported by the Health and Medical Research Fund, Food and Health Bureau, Hong Kong SAR Government (#13121412). The full report is available from the Health and Medical Research Fund website (<https://rfs1.fhb.gov.hk/index.html>).

Disclosure

The results of this research have been previously published in:

- (1) Lin D, Yan M, Lin S, Chen S. Increasing prevalence of hydrogen sulfide negative *Salmonella* in retail meats. *Food Microbiol* 2014;43:1-4.
- (2) Lin D, Chen S. First detection of conjugative plasmid-borne fosfomycin resistance gene *fosA3* in *Salmonella* isolates of food origin. *Antimicrob Agents Chemother* 2015;59:1381-3.
- (3) Wong MH, Liu L, Yan M, Chan EW, Chen S. Dissemination of IncI2 plasmids that harbor the blaCTX-M element among clinical *Salmonella* isolates. *Antimicrob Agents Chemother* 2015;59:5026-8.
- (4) Lin D, Chen K, Chan EWC, Chen S. Increasing

prevalence of ciprofloxacin-resistant food-borne *Salmonella* strains harboring multiple PMQR elements but not target gene mutations. *Sci Rep* 2015;5:14754.

- (5) Wong MH, Chan EW, Xie L, Li R, Chen S. IncHI2 plasmids are the key vectors responsible for *oqxAB* transmission among *Salmonella* species. *Antimicrob Agents Chemother* 2016;60:6911-5.
- (6) Wong MH, Xie M, Xie L, et al. Complete sequence of a F33:A-:B- conjugative plasmid carrying the *oqxAB*, *fosA3*, and blaCTX-M-55 elements from a foodborne *Escherichia coli* strain. *Front Microbiol* 2016;7:1729.
- (7) Wong MH, Chan EW, Liu LZ, Chen S. PMQR genes *oqxAB* and *aac(6')Ib-cr* accelerate the development of fluoroquinolone resistance in *Salmonella typhimurium*. *Front Microbiol* 2014;5:521.
- (8) Lin D, Xie M, Li R, Chen K, Chan EW, Chen S. IncFII conjugative plasmid-mediated transmission of blaNDM-1 elements among animal-borne *Escherichia coli* strains. *Antimicrob Agents Chemother* 2016;61:e02285-16.
- (9) Wong MH, Chan EW, Chen S. Evolution and dissemination of OqxAB-like efflux pumps, an emerging quinolone resistance determinant among members of Enterobacteriaceae. *Antimicrob Agents Chemother* 2015;59:3290-7.
- (10) Wong MH, Kan B, Chan EW, Yan M, Chen S. IncI1 plasmids carrying various blaCTX-M genes contribute to ceftriaxone resistance in *Salmonella enterica* serovar enteritidis in China. *Antimicrob Agents Chemother* 2015;60:982-9.
- (11) Lin D, Chen K, Xie M, Ye L, Chan EW, Chen S. Effect of ceftiofur and enrofloxacin on *E. coli* sub-population in pig gastrointestinal tract. *J Glob Antimicrob Resist* 2017;10:126-30.

References

1. Mastroeni P, Morgan FJ, McKinley TJ, et al. Enhanced virulence of *Salmonella enterica* serovar typhimurium after passage through mice. *Infect Immun* 2011;79:636-43.
2. Ibarra JA, Knodler LA, Sturdevant DE, et al. Induction of *Salmonella* pathogenicity island 1 under different growth conditions can affect *Salmonella*-host cell interactions in vitro. *Microbiology* 2010;156:1120-33.
3. McDermott JE, Yoon H, Nakayasu ES, et al. Technologies and approaches to elucidate and model the virulence program of salmonella. *Front Microbiol* 2011;2:121.
4. Valour F, Trouillet-Assant S, Rasigade JP, et al. *Staphylococcus epidermidis* in orthopedic device infections: the role of bacterial internalization in human osteoblasts and biofilm formation. *PLoS One* 2013;8:e67240.
5. Datsenko KA, Wanner BL. One-step inactivation of chromosomal genes in *Escherichia coli* K-12 using PCR products. *Proc Natl Acad Sci U S A* 2000;97:6640-5.

Molecular mechanisms of fluoroquinolone and expanded-spectrum cephalosporin resistance in *Vibrio parahaemolyticus*: abridged secondary publication

S Chen *, EWC Chan, KHL Po, L Ye, R Li

KEY MESSAGES

1. We investigated the molecular mechanisms of cephalosporin resistance and fluoroquinolone resistance in *Vibrio parahaemolyticus* strains isolated from food and clinical specimens.
2. Cephalosporin resistance in *V parahaemolyticus* was due to expression of β -lactamase gene, bla_{PER-1} and bla_{CMY-2} , harboured by various conjugative plasmids.
3. The complete sequence of bla_{PER-1} -bearing plasmid, pVPH1, was depicted and found to belong to the MOB_(H12) group of self-transmissible plasmids, which is prevalent in *Enterobacteriaceae* and *Vibrionaceae*.
4. Single amino acid substitution Ser⁸³Ile, in GyrA and the Ser⁸⁵Leu change in ParC, were found to be associated with fluoroquinolone-resistance in
5. Three novel *qnrVC* genes, *qnrVC5*, *qnrVC6*, and *qnrVC7*, were detectable in these strains and their structure and functions were characterised. Three novel *qnrVC* genes, *qnrVC5*, *qnrVC6*, and *qnrVC7*, were detectable in these strains and their structure and functions were characterised.

V parahaemolyticus.

Hong Kong Med J 2020;26(Suppl 4):S43-7
HMRF project number: 13121422

^{1,2} S Chen, ¹ EWC Chan, ¹ KHL Po, ¹ L Ye, ¹ R Li

¹ Department of Applied Biology and Chemical Technology, The Hong Kong Polytechnic University, Hong Kong

² Department of Infectious Diseases and Public Health, City University of Hong Kong, Hong Kong

* Principal applicant and corresponding author: shechen@cityu.edu.hk

Introduction

Vibrio parahaemolyticus is a major causative agent of gastroenteritis, particularly in areas with high seafood consumptions; *V parahaemolyticus* infection has increased owing to emergence of the serotype O3:K6.¹ Our recent study reported an increasing trend of resistance in *V parahaemolyticus* against new front-line antibiotics such as fluoroquinolones and extended-spectrum-cephalosporins. In Hong Kong, the increasing prevalence of multidrug-resistant *V parahaemolyticus* strains may impact public health because it is the leading cause of foodborne illnesses. It is important to understand the molecular mechanisms that cause *V parahaemolyticus* resistance against fluoroquinolones and extended-spectrum-cephalosporins. The current study aimed to delineate the molecular mechanisms of fluoroquinolone and extended-spectrum-cephalosporin resistance in *V parahaemolyticus*. Results may provide guidance of clinical treatment of multidrug resistant *V parahaemolyticus* and insights to developing new approaches to prevent further dissemination of multidrug resistance-encoding elements in *V parahaemolyticus*.

Methods

The isolation of *V parahaemolyticus* from food

samples was performed as previously described.² All *V parahaemolyticus* strains were cultured in LB broth or agar containing 3% salt.

Susceptibilities to 13 antimicrobials were determined by an agar dilution method according to the guidelines of Clinical and Laboratory Standards Institute.³

PCR assays for screening most of the reported β -lactamases and plasmid mediated quinolone resistance (PMQR) were performed as previously described.⁴

Bacterial genome sequencing was performed using the Illumina platform in Beijing Genome Institute. Bacterial plasmid sequencing was performed using both Illumina and PacBio platforms as previously described.⁵

Results and Discussion

Bacterial isolation

A total of 385 *V parahaemolyticus* isolates were collected from raw shrimp samples purchased in markets in four different locations (Hong Kong Island, Hung Hom, Tsuen Wan, and Sai Kung) in Hong Kong from January to April in 2010 and May to September in 2011. A total of 98 clinical *V parahaemolyticus* strains isolated from stool

samples of diarrhoeal patients collected from the Prince Wales Hospital and Beijing CDC from 2009 to 2011 were also included. A total of 54 (17%) *V parahaemolyticus* strains were isolated from various food samples in Shenzhen from 2012.

Antimicrobial resistance profile of clinical and food *V parahaemolyticus* isolates

The 385 *V parahaemolyticus* strains isolated from shrimps in Hong Kong were highly resistant to ampicillin (88%), amikacin (52%), and tetracycline (51%). The isolates also exhibited resistance to sulfamethoxazole (43%), nalidixic acid (40%), streptomycin (35%), kanamycin (32%), and chloramphenicol (30%). Surprisingly, about 9% of the *V parahaemolyticus* isolates also exhibited resistance to cefotaxime, ceftriaxone, and aztreonam, and 9% of them were resistant to ciprofloxacin. The *V parahaemolyticus* strains isolated from clinical specimens were mostly susceptible to most of the antibiotics tested. They were highly resistant to ampicillin (92%), followed by sulfamethoxazole (20%), nalidixic acid (16%), streptomycin (10%), kanamycin (8%), chloramphenicol (8%), tetracycline (6%), and ciprofloxacin (2%). No isolate was resistant to cephalosporins. The 54 *V parahaemolyticus* isolates collected from Shenzhen exhibited a high rate of resistance to ampicillin (100%) and tetracycline (11%). Five isolates (9%) were resistant

to sulfamethoxazole/trimethoprim, one isolate was resistant to chloramphenicol. Importantly, two isolates were found to be resistant to amoxicillin/clavulanic acid, cefoxitin, and ceftazidime.

Mechanisms of extended-spectrum cephalosporin resistance in *V parahaemolyticus*

Identification of β -lactamase genes

Among the *V parahaemolyticus* stains isolated from Hong Kong and Shenzhen, 21 non-repeated (maximum one isolate per sample) cephalosporin-resistant *V parahaemolyticus* strains were obtained, including 12 isolated in 2010 in Hong Kong, 7 isolated in 2011 in Hong Kong, and two isolated from Shenzhen in 2012. These cephalosporin-resistant *V parahaemolyticus* strains were further characterised to delineate their mechanisms of cephalosporin resistance. The *bla*_{PER-1} gene was identified in all these 12 isolates. For two cephalosporin-resistant *V parahaemolyticus* strains (V43 and V4) isolated from food in Shenzhen, *bla*_{TEM-1} and *bla*_{PER-1} were detected in V43, whereas the β -lactamase gene *bla*_{CMY-2} was detected for the first time in strain V4 (Table).

Characterisation of *bla*_{PER-1}-bearing plasmid

Three *bla*_{PER-1} positive isolates (V43, 2010V36, and 2011V1) that exhibited unique PFGE patterns were

TABLE. Antimicrobial susceptibility profile of *V parahaemolyticus* strains or *Escherichia coli* carrying various antimicrobial resistance genes

Strain	β -lactamase gene	Plasmid mediated quinolone resistance	Minimal inhibitory concentration, mg/L									
			AMP (32)*	CTX (4)	CRO (4)	CAZ (16)	GEN (16)	NAL (32)	CIP (4)	CHL (32)	KAN (64)	TRI (16)
J53			1	≤0.125	≤0.125	≤0.125	1	2	≤0.125	2	0.25	≤0.125
V4	<i>bla</i> _{CMY-2}		128	8	32	8	1	0.5	≤0.125	2	8	16
V4-J53	<i>bla</i> _{CMY-2}		>128	16	64	64	1	2	≤0.125	64	1	>64
V43	<i>bla</i> _{PER-1}		>128	>128	>128	>128	8	1	≤0.125	2	8	32
V43-J53	<i>bla</i> _{PER-1}		128	128	128	>128	8	2	≤0.125	32	0.5	>64
2010V36	<i>bla</i> _{PER-1}		>128	>128	>128	>128	1	0.25	≤0.125	0.25	2	16
2010V36-J53	<i>bla</i> _{PER-1}		>128	>128	>128	>128	1	2	≤0.125	2	2	>64
2011V1	<i>bla</i> _{PER-1}		>128	>128	>128	>128	4	0.5	≤0.125	16	64	>64
2011V1-J53	<i>bla</i> _{PER-1}		>128	>128	>128	>128	4	4	≤0.125	16	64	>64
<i>E coli</i> TG.1(pCR2.1)								4	<0.05			
TG.1(pCR2.1- <i>qnrVC1</i>)		<i>qnrVC1</i>						32	0.125			
TG.1(pCR2.1- <i>qnrVC6</i>)		<i>qnrVC6</i>						64	0.25			
TG.1 (pCR2.1- <i>qnrVC5</i>)		<i>qnrVC5</i>						32	0.1			
TG1(pCR2.1- <i>qnrVC7</i>)		<i>qnrVC7</i>						16	0.06			
TG1(pCR2.1- <i>qnrVC5-S100A</i>)		<i>qnrVC5</i>						32	0.25			
TG1(pCR2.1- <i>qnrVC5-A152T</i>)		<i>qnrVC5</i>						8	0.06			
TG1(pCR2.1- <i>qnrVC7-A100S</i>)		<i>qnrVC7</i>						16	0.06			
TG1(pCR2.1- <i>qnrVC7-T152A</i>)		<i>qnrVC7</i>						32	0.25			

selected for further characterisation. Conjugation experiments showed that plasmids carrying bla_{PER-1} in these three *V. parahaemolyticus* strains could be transferred to *Escherichia coli* J53. S1 nuclease PFGE and Southern hybridisation showed that the bla_{PER-1} gene in V43 and 2011V1 was located in a plasmid of ~200kb in size, and the bla_{PER-1} gene in strain 2010V36 was located in a ~175kb plasmid. The complete sequence of plasmid from a *V. parahaemolyticus* strain V36, designated as pVPH1, was obtained. The complete plasmid sequence of pVPH1(KP688397) was 183,730bp in size and had an average G+C content of 45.2%, which is similar to that of the chromosome of *V. parahaemolyticus* (45.1% to 45.6%). Annotation results revealed that pVPH1 harboured 114 predicted coding sequences; among them, several functional regions could be identified. After conducting the BLASTN alignment search against NCBI database, the sequence organisation of pVPH1 was found to be similar to that of pAQU1 (72%) and pAQU2 (76%) [Fig 1]. The MDR regions of pVPH1 are centralised in a region of ~40kb in size, which is flanked by two different Tn3 family transposase genes. There were many different genetic mobile elements in this mosaic region, such as IS26, Class 1 Integron, ISCR1, IS4321 and IS6100. A mercuric resistance operon (*mer* operon) was also found between the Tn3 and the TniA transposase elements, which was similar to that of plasmid pR148 from *Aeromonas hydrophila*. Downstream of the mercuric resistance operon was a ParDE type II toxin-antitoxin system. A Class 1 Integron with an *arr3-dfrA23* cassette flanked by IS26 and ISCR1 was

also found with bla_{PER-1} being located downstream of ISCR1 in an area including *gst* (encoding a glutathione S-transferase), *abct* (encoding an ABC-type transporter) and three hypothetical genes, followed by the *qacEΔ1* and *sul1* genes. This mobile element can be circularised, and it was speculated that ISCR1 may act like IS91 to generate circular intermediates and mobilise genes immediately upstream of ISCR1.

Characterisation of bla_{CMY-2} -bearing plasmid by S1-PFGE and Southern hybridisation

Conjugation experiments showed that the plasmid borne bla_{CMY-2} gene in V4 strain could be transferred to *E. coli* J53. S1 nuclease PFGE and Southern hybridisation analysis showed that the V4 strain harboured 4 plasmids of different sizes, ranging from ~45kb to ~150kb. The conjugative plasmid detected in transconjugant V4J53 was ~150kb in size. Southern hybridisation confirmed that the bla_{CMY-2} gene was located in this transmissible plasmid in both V4 and V4J53. Plasmid typing indicated that the transmissible plasmid belonged to IncA/C type plasmid.

The flanking sequence of bla_{CMY-2} was amplified by PCR mapping according to published sequences and confirmed by sequencing. It was found that the arrangement of genetic environment of bla_{CMY-2} was *traB-traV-traA-ISEcp1-bla_{CMY-2}-blc-sugE-encR-orf1-orf2-orf3-orf4-dsbC-traC* (Fig 1). The β -lactamase gene bla_{CMY-2} gene is the most commonly reported plasmid-encoded AmpC β -lactamase gene in *Salmonella* spp, *E. coli*, and other

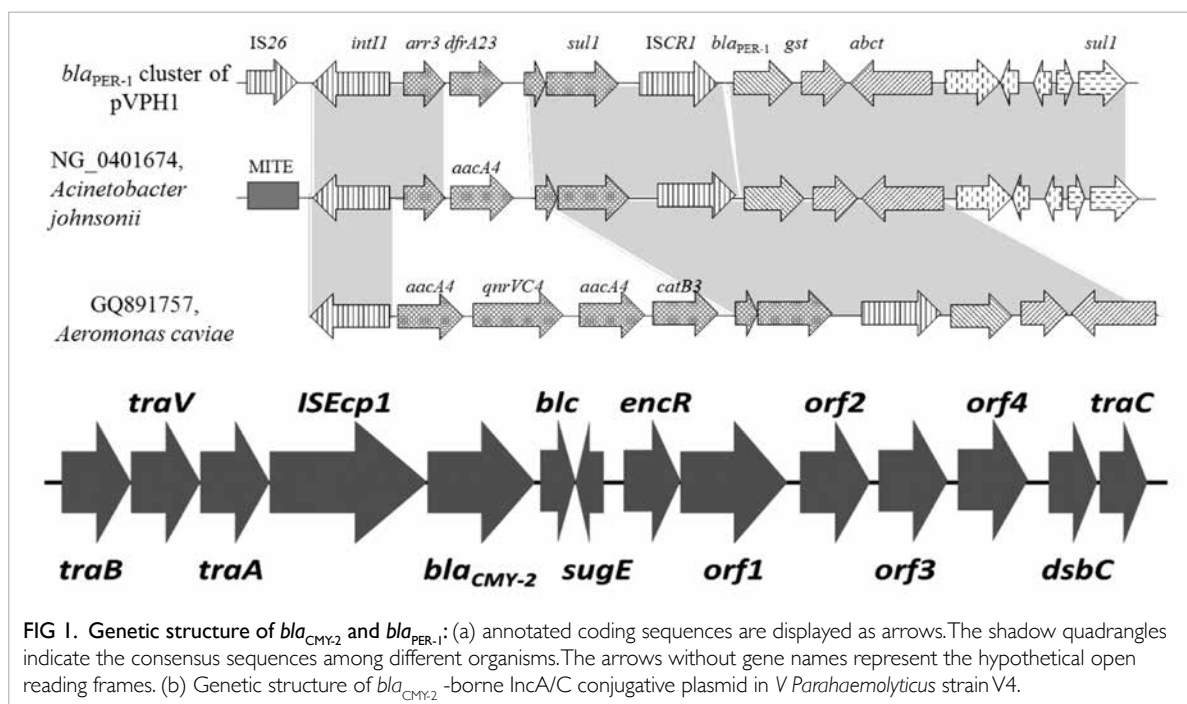


FIG 1. Genetic structure of bla_{CMY-2} and bla_{PER-1} : (a) annotated coding sequences are displayed as arrows. The shadow quadrangles indicate the consensus sequences among different organisms. The arrows without gene names represent the hypothetical open reading frames. (b) Genetic structure of bla_{CMY-2} -borne IncA/C conjugative plasmid in *V. Parahaemolyticus* strain V4.

species of *Enterobacteriaceae* worldwide. This gene renders the host organisms resistant to a variety of β -lactams, including oxyimino-cephalosporins and cephamycins.

Mechanisms of quinolone/fluoroquinolone resistance in *V parahaemolyticus*

Mechanisms of quinolone resistance

A total of 65 nalidixic-acid-resistant, ciprofloxacin-susceptible *V parahaemolyticus* strains isolated

from Hong Kong from 2010-2011 were selected to investigate the mutations in *gyrA* and *parC* genes and the presence of plasmid-mediated quinolone resistance (PMQR) genes. Most quinolone-resistant isolates were found to possess a single mutation which resulted in the S83I amino acid change in GyrA (77%), among which 62% harboured another single mutation which resulted in the S85F substitution in ParC. Around 23% of the nalidixic acid-resistant did not possess any target mutations, suggesting that other mechanisms of quinolone resistance were involved. However, none of the known PMQR genes including *qnr*, *qeqA*, *oqxAB*, or *qnrVC* was detectable in any of these strains.

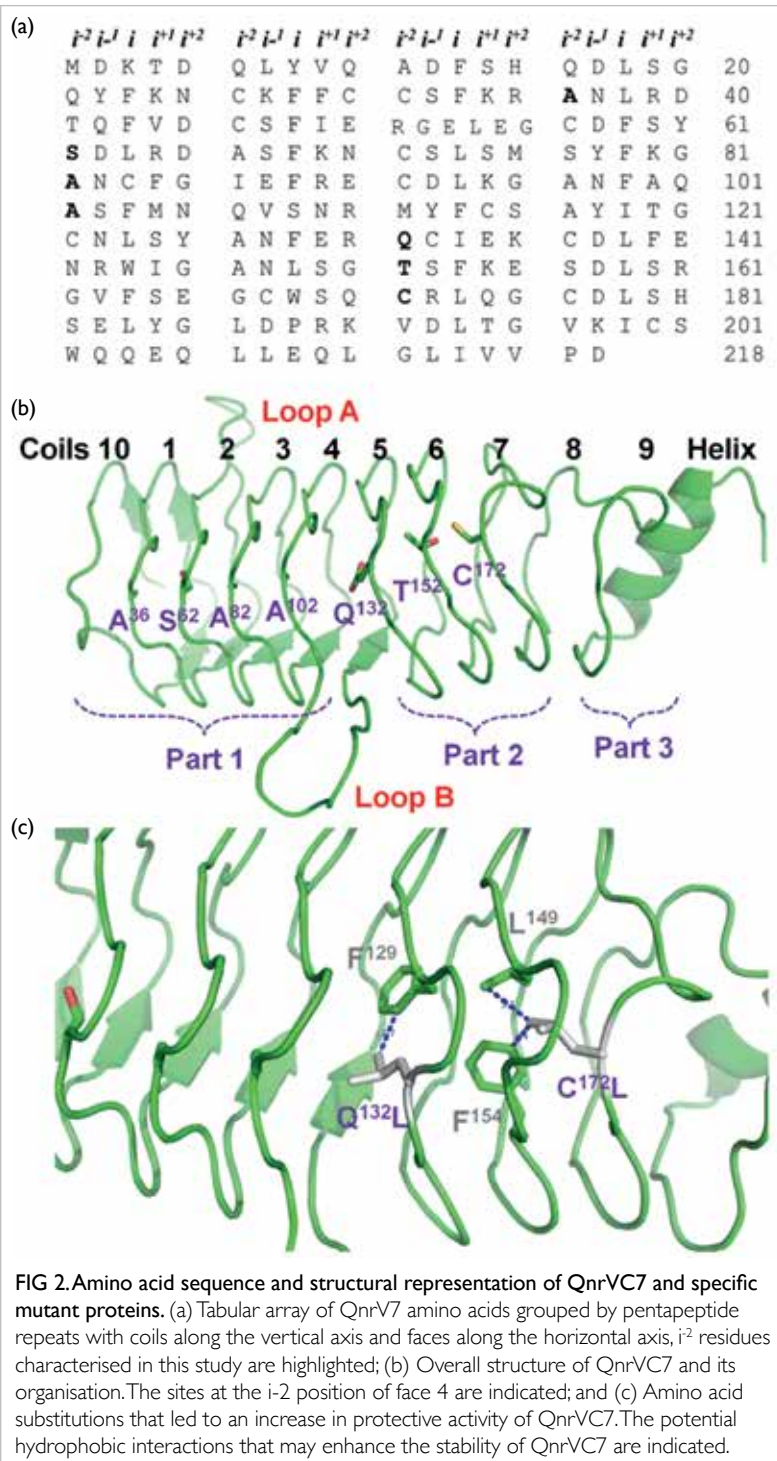
Mechanisms of fluoroquinolone resistance and novel PMQR genes in *V parahaemolyticus*

Fifteen non-repeated (maximum one isolate per sample) ciprofloxacin-resistant *V parahaemolyticus* strains (minimal inhibitory concentration [MIC] ≥ 4) isolated from shrimp samples in 2010 were selected to characterise their molecular mechanism of fluoroquinolone resistance. All isolates except for one were found to harbour the single amino acid substitution Ser⁸³Ile, in GyrA and Ser⁸⁵Leu change in ParC (Table). The actual contribution of single amino acid substitution in GyrA and ParC to fluoroquinolone resistance in *V parahaemolyticus* needs further confirmation since mutations in both genes have also been found to be associated with only intermediate resistance to ciprofloxacin in *V cholera* isolates. One *V parahaemolyticus* isolate was resistant to norfloxacin, but did not harbour any mutations in both *gyrA* and *parC* genes, or any known PMQR genes.

A new *qnrVC* gene with a novel substitution, Ala¹⁰⁰Ser, compared to *qnrVC4*, was identified. We designated this novel *qnrVC* gene as *qnrVC5*. To further confirm its functional role, the whole coding region of *qnrVC5* and its natural promoter region were cloned into the pCR2.1 vector using primers. The MIC of *E coli* carrying the pCR2.1-*qnrVC5* exhibited reduced susceptibility to ciprofloxacin (MIC=0.1) and resistance to nalidixic acid (MIC=32) [Table].

Another novel *qnrVC* gene, *qnrVC6*, was detected in a ~200kb conjugative plasmid that also carried a *bla*_{PER-1} gene recovered from a *V parahaemolyticus* strain isolated from food. Sequence analysis of the full length *qnrVC* gene revealed that this gene differed from *qnrVC1* by one single amino acid, Asp⁷¹Asn. Cloning of this novel *qnrVC* allele as *qnrVC6* mediated decreased susceptibility to ciprofloxacin and nalidixic acid, suggesting a role of *qnrVC6* in mediating nalidixic acid resistance (Table).

A novel *qnrVC*-like gene was identified in one *V cholerae* isolate. Sequence analysis of the



full-length of this gene showed that it differed from *qnrVC5* by three amino acids substitution (M¹⁸L, S¹⁰⁰A and A¹⁵²T). We designated this novel *qnrVC* allele as *qnrVC7*. The activities of the *qnrVC* gene product were investigated by determining the MICs to fluoroquinolones/quinolones of the clone. *E coli* TG1 carrying pCR2.1-*qnrVC7* exhibited reduced susceptibility to ciprofloxacin and nalidixic acid (Table). However, compared to *qnrVC5*, *E coli* carrying *qnrVC7* exhibited ~2-fold and 4-fold lower MIC toward nalidixic acid and ciprofloxacin respectively. Mutational analysis of various residues between revealed that substitution of A¹⁵² by T reduced the activity of the *qnrVC7* product and A¹⁵² was critical for the activity of QnrVC proteins.

Structural and functional characterisation of QnrVC7 protein

Sequence comparison and mutational analysis showed that amino acid T¹⁵², located at the i⁻² position on face 4, was responsible for the reduced protection activity of QnrVC7. This study extended the characterisation to all residues located at the i⁻² position of face 4 to elucidate the structure / activity relationship of QnrVC7 as well as other Qnr proteins. These data suggested that Ala, Ser and in some cases Thr were the best fit residues at i⁻² position of face 4 on coils 1, 2, 3 and 4, and that the bulky side chain residues such as Leu and Asp would disrupt the well-organised tight stacks of these coils. The requirement of small side chain residues at i⁻² position was consistent with the finding in other Qnrs such as QnrA and QnrC. However, substitution with Gly was not tolerated either, suggesting the small side chain is required for forming the stable stack between coils (Fig 2).

Funding

This study was supported by the Health and Medical Research Fund, Food and Health Bureau, Hong Kong SAR Government (#13121422). The full report is available from the Health and Medical Research Fund website (<https://rfs1.fhb.gov.hk/index.html>).

Disclosure

Results from this research project have been published in:

- (1) Li R, Chiou J, Chan EW, Chen S. A novel PCR-based approach for accurate identification of *Vibrio parahaemolyticus*. *Front Microbiol* 2016;7:44.
- (2) Li R, Lin D, Chen K, Wong MH, Chen S. First detection of AmpC β-lactamase bla(CMY-2) on a conjugative IncA/C plasmid in a *Vibrio parahaemolyticus* isolate of food origin. *Antimicrob Agents Chemother* 2015;59:4106-11.
- (3) Chiou J, Li R, Chen S. CARB-17 family of β-lactamases mediates intrinsic resistance to penicillins in *Vibrio parahaemolyticus*. *Antimicrob Agents Chemother* 2015;59:3593-5.
- (4) Liu M, Wong MH, Chen S. Molecular characterisation of a multidrug resistance conjugative plasmid from *Vibrio parahaemolyticus*. *Int J Antimicrob Agents* 2013;42:575-9.
- (5) Liu M, Chen S. Draft genome sequence of *Vibrio parahaemolyticus* V110, isolated from shrimp in Hong Kong. *Genome Announc* 2013;1: pii:e00300-13.
- (6) Wong MH, Liu M, Wan HY, Chen S. Characterization of extended-spectrum-β-lactamase-producing *Vibrio parahaemolyticus*. *Antimicrob Agents Chemother* 2012;56:4026-8.
- (7) Liu M, Wong MH, Chen S. Mechanisms of fluoroquinolone resistance in *Vibrio parahaemolyticus*. *Int J Antimicrob Agents* 2013;42:187-8.

References

1. Matsumoto C, Okuda J, Ishibashi M, et al. Pandemic spread of an O3:K6 clone of *Vibrio parahaemolyticus* and emergence of related strains evidenced by arbitrarily primed PCR and toxRS sequence analyses. *J Clin Microbiol* 2000;38:578-85.
2. Wong MH, Liu M, Wan HY, Chen S. Characterization of extended-spectrum-β-lactamase-producing *Vibrio parahaemolyticus*. *Antimicrob Agents Chemother* 2012;56:4026-8.
3. Institute CaLS. Performance standards for antimicrobial susceptibility testing. Eighteen informational supplement (M100-S18). Wayne, PA: Clinical and Laboratory Standards Institute; 2008.
4. Kumarasamy KK, Toleman MA, Walsh TR, et al. Emergence of a new antibiotic resistance mechanism in India, Pakistan, and the UK: a molecular, biological, and epidemiological study. *Lancet Infect Dis* 2010;10:597-602.
5. Ye L, Li R, Lin D, et al. Characterization of an IncA/C multidrug resistance plasmid in *Vibrio alginolyticus*. *Antimicrob Agents Chemother* 2016;60:3232-5.

AUTHOR INDEX

Au SWN	29, 32	Li R	39, 43
Chan EWC	39, 43	Lin D	39
Chan MCW	8	Nelson EAS	8
Chan PKS	8	Ng IOL	22
Chan VSF	32	Ngo JCK	29
Chen S	39, 43	Nim YS	29
Ching RHH	22	Peiris JSM	12, 17
Chiu SSS	12	Po KHL	43
Chiu YT	22	Soares Magalhaes RJ	12
Cho CH	26	Sze KH 35	
Clements ACA	12	Sze KMF 22	
Cowling BJ	4, 17	Tam CL	29
Hu W	26	Thach TQ	12
Hu WB	12	Wong CM	12
Huang P	29	Wong KB	29
Ip DK	4	Wong MHY	39
Kao RYT	35	Wu P	17
Lam WL	32	Wu WKK	26
Lau EYT	22	Xu YF	29
Lau KF	32	Yang L	12
Lee JMF	22	Ye L	43
Lee TKW	22	Yen HL	4
Leung TF	8	Yuen MH	29
Li M	32	Zhang L	26

Disclaimer

The reports contained in this publication are for reference only and should not be regarded as a substitute for professional advice. The Government shall not be liable for any loss or damage, howsoever caused, arising from any information contained in these reports. The Government shall not be liable for any inaccuracies, incompleteness, omissions, mistakes or errors in these reports, or for any loss or damage arising from information presented herein. The opinions, findings, conclusions and recommendations expressed in this publication are those of the authors of the reports, and do not necessarily reflect the views of the Government. Nothing herein shall affect the copyright and other intellectual property rights in the information and material contained in these reports. All intellectual property rights and any other rights, if any, in relation to the contents of these reports are hereby reserved. The material herein may be reproduced for personal use but may not be reproduced or distributed for commercial purposes or any other exploitation without the prior written consent of the Government. Nothing contained in these reports shall constitute any of the authors of these reports an employer, employee, servant, agent or partner of the Government.

Published by the Hong Kong Academy of Medicine Press for the Government of the Hong Kong Special Administrative Region. The opinions expressed in the *Hong Kong Medical Journal* and its supplements are those of the authors and do not reflect the official policies of the Hong Kong Academy of Medicine, the Hong Kong Medical Association, the institutions to which the authors are affiliated, or those of the publisher.